Materials Horizons

ROYAL SOCIETY OF CHEMISTRY

REVIEW

View Article Online
View Journal | View Issue

Cite this: *Mater. Horiz.*, 2023, **10**, 3269

Bio-inspired artificial synaptic transistors: evolution from innovative basic units to system integration

Xin Wang,[a] Yixin Ran,[a] Xiaoqian Li,[b] Xinsu Qin,[a] Wanlong Lu,[a] Yuanwei Zhu [a] and Guanghao Lu *[a]

Received 14th February 2023,
Accepted 9th May 2023

DOI: 10.1039/d3mh00216k

rsc.li/materials-horizons

The investigation of transistor-based artificial synapses in bioinspired information processing is undergoing booming exploration, and is the stable building block for brain-like computing. Given that the storage and computing separation architecture of von Neumann construction is not conducive to the current explosive information processing, it is critical to accelerate the connection between hardware systems and software simulations of intelligent synapses. So far, various works based on a transistor-based synaptic system successfully simulated functions similar to biological nerves in the human brain. However, the influence of the semiconductor and the device structural design on synaptic properties is still poorly linked. This review concretely emphasizes the recent advances in the novel structure design of semiconductor materials and devices used in synaptic transistors, not only from a single multifunction synaptic device but also to system application with various connected routes and related working mechanisms. Finally, crises and opportunities in transistor-based synaptic interconnection are discussed and predicted.

1. Introduction

The concept of mimicking brain computing using neuromorphology was put forward in the late 1980s, motivated by the human brain which has an efficient information processing ability.[1,2] Unlike von Neumann-based storage separation computing architecture, biological nervous systems possess efficient parallel calculations, ultralow power consumption and high fault tolerance superiority.[3–6] In a typical case, AlphaGo, built with only 1200 central processing units (CPUs) and 180 graphics processors (GPUs), could generate hundreds of thousands of watts of power. Biologically, the difference is the power consumption as low as 20 watts when processing information by the brain which contains 10^{11} neurons and 10^{15} synapses.

[a] *Frontier Institute of Science and Technology, State Key Laboratory of Electrical Insulation and Power Equipment, Xi'an Jiaotong University, Xi'an 710054, P. R. China. E-mail: guanghao.lu@mail.xjtu.edu.cn*
[b] *Shandong Technology Center of Nanodevices and Integration, School of Microelectronics, Shandong University, Jinan, Shandong Province, 250100, P. R. China*

Xin Wang

Xin Wang is currently a PhD candidate in Xi'an Jiaotong University (XJTU), China. She received her bachelor's degree in 2018 from Taiyuan University of Science and Technology and MS degree in 2021 from Zhengzhou University. Her research interests focus on the preparation and application of flexible, low power consumption and multi-function intelligent synapse devices, memory devices and logic circuit.

Yixin Ran

Yixin Ran is currently pursuing his MS degree at the Institute of Frontier Science and Technology, Xi'an Jiaotong University, China. He received his BSc in Materials Science and Engineering from Hunan University, China, in 2017. His research interests focus on the study of optical and electrical distributions in organic semiconductor thin films and the preparation of high-performance multifunctional organic semiconductor optoelectronic devices.

Similar to biological synapses, artificial synaptic devices that can simultaneously perform information processing and storage functions are considered a promising way to achieve brain-like computing. Therefore, there is a high demand for brain-like chip technology constructed by artificial synaptic devices to promote the evolution of artificial intelligence, sensor interconnection, human-computer interaction and efficient storage computing of explosive information.[7–9] Individual intelligent synaptic devices and sensing interconnect systems are expected to open the door of new-generation intelligent neurorobotics.[10–12]

In addition, inspired by the brain, an ultra-low-power efficient computing system,[13] scientists are planning to design a low-power brain-like computer with efficient computing ability to break through the limitations of power walls in the post-Moore era.[14,15] To achieve this goal, two mainstream techniques involving complementary metal oxide semiconductor (CMOS) based hardware digital systems and an intelligent synaptic software system have been widely studied.[14,16–18] However, digital circuits based on CMOS technology are limited by Moore's Law to exhibit megawatt-standard energy consumption, which is far more than the human brain (20 W).[19–21] Therefore, new hardware architectures such as coherent nanophotonic circuits and quantum neural network,[22,23] novel neural network integration systems such as self-powered neural devices, zero-gate neural devices,[24,25] *etc.* have been designed to meet the low-power requirements of industry and academia.[26,27]

Recently, diverse materials including organic semiconductors,[28] oxide semiconductors,[29] carbon nanotubes,[30] two-dimensional materials,[31] quantum dots,[32] multiple composite materials,[33] and device structures mainly focus on two-terminal[34] and three-terminal devices,[35] which have been attempted to fabricate a synaptic system. Additionally, an artificial intelligence network is introduced to imitate more complex features with low power consumption.[15,36] Compared with two-terminal devices like memristors, atomic switches and phase change memories,[37,38] three-terminal transistors possess higher fault tolerance, higher signal-to-noise ratio and a greater signal modulation property.[39–41] Mainstream neuronal synaptic transistors cover both vertical structures and planar structures, and the channel length could be regulated more accurately by vertical structure transistors and thus achieve a low power consumption.[42,43] According to the different implementation principles of synaptic transistors, they can be divided into polyelectrolyte,[44] ion-gel,[45] floating-gate,[46] electret,[47]

Xiaoqian Li

Li Xiaoqian is currently a PhD candidate at the School of Microelectronics of Shandong University, majoring in microelectronics and solid-state electronics. She received her BS degree from Qufu Normal University (2018). She obtained an MS degree in materials science and engineering from Zhengzhou University (2021). Her research interests are the fabrication and developments of artificial synapses and neurons by means of diverse functional material systems.

Xinsu Qin

Xinsu Qin is currently pursuing her MS degree at the School of Chemistry, Xi'an Jiaotong University, China. She received her BSc in Forestry Products and Chemical Engineering from Northeast Forestry University, China, in 2016. Her research interests focus on the preparation of organic blend thin film devices and high-performance multifunctional organic semiconductor optoelectronic devices.

Wanlong Lu

Wanlong Lu is a PhD candidate at Xi'an Jiaotong university under the direction of Dr Guanghao Lu. His study is centered on developing new organic semiconductor materials for high performance photoelectric devices.

Yuanwei Zhu

Dr Yuanwei Zhu is currently an associate professor at the school of electrical engineering in Xi'an Jiaotong University (XJTU), China. He received the PhD degree in electrical engineering from XJTU in 2018. His research interests include dielectrics, electrical insulating materials, organic semiconductors and their applications in power equipment and electronic devices. He can be reached at zhuyuanwei@.xjtu.edu.cn.

ferroelectric,[48] polarized type and heterojunction structure transistors.[49,50] Based on these materials and structures, diverse artificial synapse devices and neural networks (ANNs) are developed for different information transfer and simulation applications. For example, stretchable flexible and wearable synaptic electronic systems implemented by printing technology are being vigorously developed with the advantages of organic semiconductors and carbon nanotubes that can be easily dissolved and printed.[51–54] Using typical printing techniques such as intaglio printing, screen printing, and roll-to-roll printing it is easier to realize high-throughput printing patterns, however, the specific mask and ink viscosity needs to be carefully designed.[55] Inkjet printing, as a layer-by-layer printing technology without a mask, can not only print multilayer complex patterns but also realize high-resolution patterns more easily.[8] In addition, inorganic semiconductors possess a higher carrier mobility and can be applied to high-frequency electronic circuits,[56] while quantum dots and heterojunctions have higher sensitivity to light and are suitable for optical synaptic systems.[57,58] Additionally, some biocompatible synaptic devices especially the organic transistors can be degraded without any pollution and toxicity, which further facilitates the convergence of biotechnology and electronics in recording potential information from neurons.[59,60]

Until now, major biological synaptic functions such as excitatory/inhibitory postsynaptic current (EPSC/IPSC), short/long term plasticity (STP/LTP) and paired pulse facilitation (PPF) have been widely simulated by controlling presynaptic stimulation.[61] In addition, a more advanced evolution of synaptic transistors towards complex functions and system integration are extensively studied to enrich the diversity of signal transmission and perception processes.[62–64] Multiple inputs gates represent different environment signals to reflect the changes of surroundings and keep a memory of changing information through intelligent bionic systems. Furthermore, coupling vision system simulations to the human eye, tactile sensing systems to robot movement, auditory nervous system to human ears and the combination of a triboelectric system with muscle movement are currently being researched to reflect real-time dynamic changes in external information.[65–69]

Guanghao Lu

Guanghao Lu, PhD, professor. He received his bachelor's degree in 2004 from Nanjing University and PhD degree in 2010 from Changchun Institute of Applied Chemistry, Chinese Academy of Sciences. After postdoctoral research in Germany and afterwards in the USA from 2010 to 2014, he joined Frontier Institute of Science and Technology, Xi'an Jiaotong University. The research of his group focuses on polymer thin film semiconductors and electronics.

However, as the increasing data needs to be stored and recorded in the information age, multiple sensors are required, including acoustic, thermal, optical, electrical, strain and other coupling interconnections. In addition, the design of material systems, efficient calculation, operating power consumption and related working mechanism also need to be further optimized.[70–73] Therefore, the incorporation of sensing, conveying, simulating and feedback of information in single devices or synaptic systems are facing enormous challenges to the realization of related artificial intelligence.

Herein, recent advances in intelligent synaptic devices and system integration applications are discussed with respect to strategies for designing structures of materials and transistors, and coupling of various multifunctional devices and neuronal systems. Fig. 1 exhibits the main framework of this review. We highlight the effect of innovative structure design in materials and devices on the application of intelligent synaptic transistors in Section 2, multifunctional synaptic device including stretchable, degradable and multi-mode reconfigurable devices in Section 3 and the integration of artificial nervous systems in Section 4. These contents establish a foundation for hardware implementation of neuromorphic transistors and their applications in human vision, robot movement and self-powered devices. Potential mechanism of information transfer and challenges based on neuromorphic systems are also discussed in detail, which might give these devices emotional/operative attributes. Finally, the materials, high-throughput preparation techniques, multifunctional devices and multifunctional simulations commonly used in synapses were are summarized in Fig. 12. It is believed that the development of multimodal intelligent synaptic systems and brain-like chips would open a new chapter in artificial intelligence, wearable and stretchable electronic skin for constructing Internet of Everything and brain-like computing systems with perceptual intelligence.

2. Innovative structures of materials and transistors for smart synapses

Recently, proliferating research about transistor-based smart synapses undoubtedly accelerated the development of neuroelectronics. Among which, the structure of materials and devices shows significant impacts on the synaptic functions. Semiconductor materials used for smart synapse construction such as organic, metal oxides, carbon nanotubes, 2D materials, composite heterojunctions, phase-change materials *etc.* and devices mainly focus on a planar structure with floating gate, electret, ferroelectric and electrochemical mechanisms, both of which have been summarized carefully in related reviews.[41,80–82] However, there are few reviews on the effects of specific structures of semiconductor materials and devices on synaptic properties. This subsection focuses on establishing the effects of novel designs of semiconductor materials (mainly including nanofibers, nanoparticles, single crystal combine with fiber structuring engineering, nanosheets, and dendritic network *etc.*) and device structures on synaptic properties. The

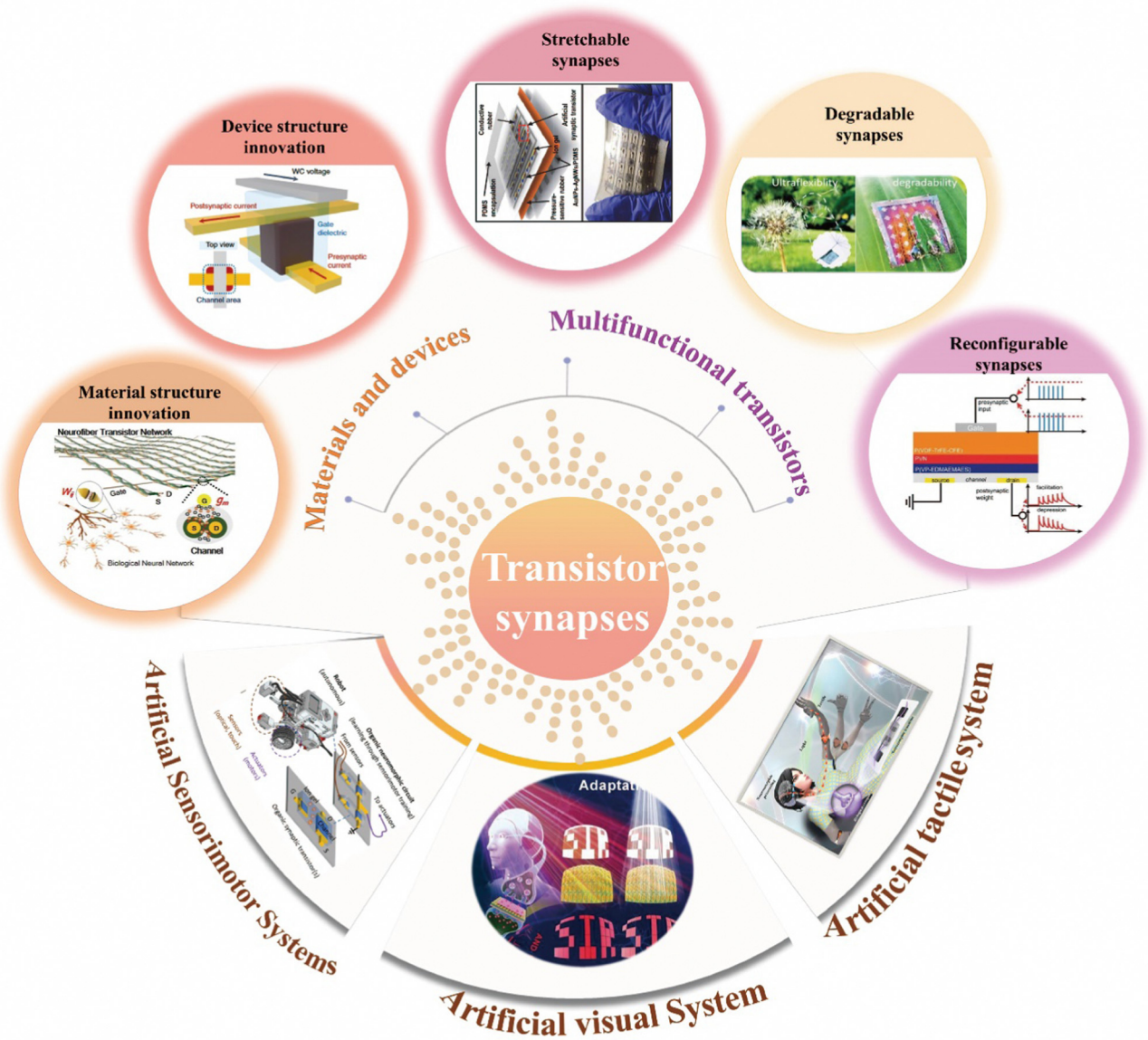

Fig. 1 Summary of this review regarding transistor-based synapse researches. Organic synapse neuro-nanofiber transistors based on a dendritic network. Reproduced with permission.[74] Copyright 2021, Wiley-VCH. Three-dimensional crossbar organic synaptic device utilizing a vertical structure. Reproduced with permission.[75] Copyright 2020, Nature. Stretchable integrated tactile sensor skin based on an ion gel dielectric. Reproduced with permission.[76] Copyright 2019, American Association for the Advancement of Science. Degradable organic synapses natural polysaccharides. Reproduced with permission.[59] Copyright 2020, Wiley-VCH. Reconfigurable synaptic devices based on electrochemical-electret. Reproduced with permission.[77] Copyright 2022, Wiley-VCH. Artificial tactile system based on gesture recognition. Reproduced with permission.[78] Copyright 2022, American Chemical Society. Artificial visual system constructed with short-wave infrared synaptic phototransistor. Reproduced with permission.[79] Copyright 2022, Wiley-VCH. Information processing based on sensorimotor integration and robotics learning. Reproduced with permission.[69] Copyright 2021, American Association for the Advancement of Science.

related materials, structures, and properties of synaptic devices are summarized in Table 1.

2.1. Novel design of material structure

Tremendous semiconductor materials have been constructed towards artificial synapses. Three operation mechanisms are generally mastered, carrier induction,[35] capture,[83] exciton generation and then separation,[84] which has been widely investigated and summarized in recent reviews.[39,85] The relationship between the special structural design of semiconductor materials (like nanofibers, nanoparticles, and single crystals combined with fiber structuring engineering, nanosheets, and dendritic networks, not the morphology of the material) and synaptic properties is the main subject in this section. Back in 2013, Shi *et al.*[86] prepared synaptic transistors with multilevel analogue states with control over the composition in ionic liquid-gated devices. In 2020, benefiting from the low conductivity and the anisotropy of selenium nanosheets, Chai *et al.*[87]

Table 1 Summary of the structure and properties of synaptic transistors

Device structure	Active layer and structure	Dielectric	Power consumption	Stimuli	Synaptic function	Synaptic properties	Ref.
Vertical	PDPP4T	SiO_2	1.3 fJ	L-Spikes	Image processing	EPSC, LTP, STP, PPF	43
Dendritic network	P3HT and P3CT neurofibers	EMIM:TFSI	—	V-Spikes	SNN	Multilevel memory, LTP, long-term stability	74
Vertical (gate-all-around)	P3HT	PVdF-HFP + EMIM:TFSI	—	V-Spikes	SNN	EPSC, IPSC, LTP/D, STP/D, PPF	75
SG	Trigonal selenium nanosheet	SiO_2	0.1 pJ	V-Spikes	Biological axon−multisynapse system simulation	EPSC, IPSC, PPF	87
TG	PEDOT:PSS/PAAm nanofibers	PDMS	113 fJ	V-Spikes	SNN	EPSC, IPSC, LTD, LTP	88
BG	Rubrene single-crystalline nanoribbons	PVA/GO	0.29 fJ	V-Spikes	High-pass filtering	EPSC, IPSC, PPF, STP, LTP	89
BG	IGZO	Bovine milk	—	V-Spikes	High-pass filtering, AND Logic	EPSC, PPF	90
BG	IGZO	Casein	—	V-Spikes	SNN	EPSC, PPF, STDP, LTD, LTP	91
BG	PDPP4T	SiO_2	—	L-Spikes	SNN	EPSC, PPF, LTP	92
EG and BG	PBDTTT-C-T	P(VDF-TrFE)	—	V and L-spikes	Simultaneous sensing of a neuro-transmitter and light	EPSC, PPF	93
TG	Poly pyrrole-fibrous	Ion-gel	0.85 pJ	V-Spikes	—	EPSC, IPSCPPF, PPD, STP	94
BG	Biocompatible graphene	PMMA	50 aJ	V-Spikes	SNN	EPSC	95
BG	InZnO	Chitosan-based biopolymer	—	V-Spikes	Synaptic filtering	EPSC, PPF	96
BG	DNTT	Poly-saccharides	—	V-Spikes	—	EPSC, STP, LTP	97
BG	PDVT-10/PC61BM heterojunction	SiO_2	—	V-Spikes	—	EPSC, IPSC, PPF	98
BG	MoS_2/PTCDA heterojunction	SiO_2	—	V and L-spikes	Synaptic filtering	EPSC, IPSC, LTP/D, STP/D, PPF	99

Notes: the vertical structure refers to the source-drain electrode position. BG, TG, SG and EG represent the bottom gate configurations, top gate configurations, side gate configurations and extended gate configurations, respectively. V-Spikes and L-spikes represent voltage spikes and light spikes, respectively. PAAm represents polyacrylamide, PDMS represents polydimethylsiloxane, PBDTTT-C-T represents poly[[4,8-bis[5-(2-ethylhexyl)-2-thienyl]benzo[1,2-*b*:4,5-*b*′]dithiophene-2,6-diyl][2-(2-ethyl-1-oxohexyl)thieno[3,4-*b*]thiophenediyl]], and IGZO represents indium-gallium-zinc oxide. SNN represents spiking neural network learning, PDVT-10 represents poly[2,5bis(alkyl)pyrrolo[3,4-*c*]pyrrolo-1,4(2*H*,5*H*)-dione-*alt*-5,5-di(thiophene2-yl)-2,2-(*E*)-2-(2-(thiophen-2-yl)-vinyl)thiophene] (PDVT-10), PC61BM represents phenyl C61 butyric acid methyl ester, MoS_2 represents molybdenum disulfide (MoS_2), PTCDA represents perylene-3,4,9,10-tetracarboxylic dianhydride, STP represents short-term plasticity, LTP represents long term plasticity, IPSC represents inhibitory post-synaptic current, EPSC represents excitatory post-synaptic current, PPD represents paired-pulse depression, and PPF represents paired pulse facilitation.

demonstrated anisotropic and low-energy synaptic transistors (less than 0.1 pJ per spike) based on trigonal selenium (t-Se) nanosheets, which offer the potential to process complex signals. Furthermore, to obtain low-power neuromorphic computing and a high-speed response, nanofiber channels with an ion-blocking layer are introduced to transistor synapses (Fig. 2a).[88] Thanks to the nanofiber architecture, the synapse shows low power consumption (113 fJ per spike, Fig. 2b) and operates up to 13.5 kHz. Notably, the energy consumption of monosynaptic events was further reduced by the combination of rubrene a single-crystalline active layer and nanoribbon structure (Fig. 2c).[89] Fig. 2d shows the minimum energy consumption of an artificial synapse is 0.29 fJ, which is much lower than biological synapses (Fig. 2e), In addition, the devices can be conformed on the head of a weevil without any crevices (Fig. 2f). Further optimized ultra-low energy-consumption (Fig. 2g) through single crystal and fiber structuring engineering offer meaningful guidance toward flexible low power intelligent neural computing. At another level, improved memory cyclic endurance and successful speech recognition for spatio-temporal iterative learning are realized utilizing dendritic network and neuro-fiber transistors, whose dendritic network structure is more similar to the biological neural network structure (Fig. 2h).[74] The architecture of electrode microfibers, ion-gel dielectric insulators and polythiophene semiconductors not only provides stable multilevel memory traits but also enhanced cyclic endurance by effectively controlling the ion doping and de-doping process under an increased network contact interface (Fig. 2i). These results supplied a strong demonstration that the design of the material structure in sheets or nanofibers can improve the response characteristics of the smart synapses such as stability, multi-state storage, and especially power consumption reduction benefiting from the low conductivity and better contact interface. Therefore, the design concept of channel materials opens blazing trails for energy-efficient neurocomputing/sensing platforms. These findings further indicate the relationships between the structure of semiconductor materials and corresponding synaptic performance, which can be used to design material structures according to the target synaptic properties in the future. However, some challenges, such as the complex preparation processes of special material structures, high costs, *etc.*, still need to be solved.

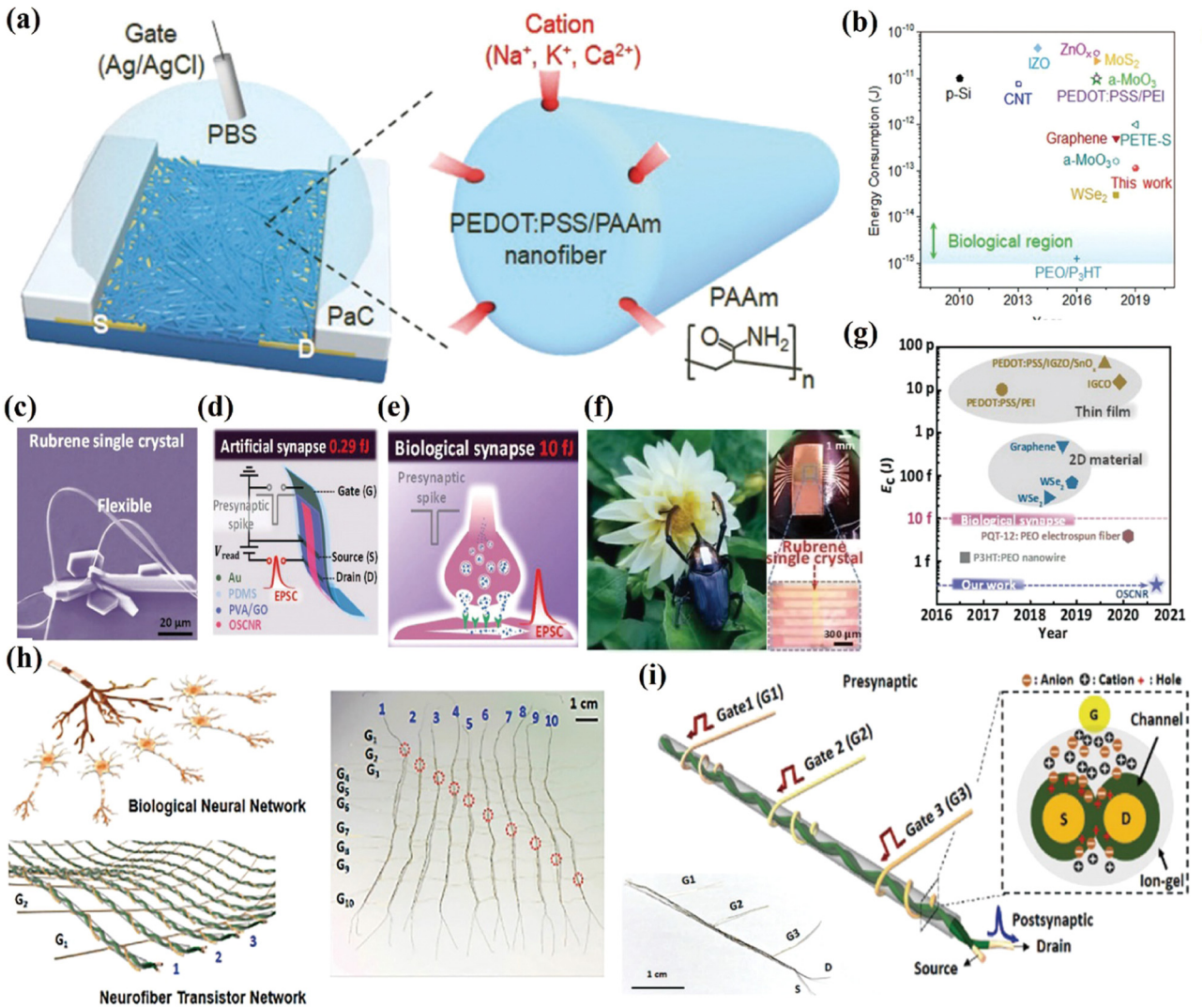

Fig. 2 New material structure for synaptic transistors with improved synapse property. (a) Schematic of the nanofiber channel of a transistor. (b) Comparison of power consumption in other synaptic devices. Reproduced with permission.[88] Copyright 2021, Wiley-VCH. (c) SEM images of a rubrene single crystal. (d) Structure illustration of a synaptic transistor. (e) Schematic of biological synapses. (f) Photograph images of the devices conformed on the head of a weevil. (g) Comparison of power consumption associated in other synaptic devices. Reproduced with permission.[89] Copyright 2021, Wiley-VCH. (h) Schematic of a biological neural network and neuro-fiber transistor. (i) Illustration of the neuro-nanofiber transistor architecture and doping mechanism in a semiconductor (inset). Reproduced with permission.[74] Copyright 2021, Wiley-VCH.

2.2. Novel device structure and working mechanism

In addition to the effect of the material structure on synaptic properties, the transistor structure also plays a crucial role in synaptic properties and the corresponding synaptic function. This section focuses on the exploration of the relationships between transistors structure and synaptic performance, including vertical synaptic transistors, planar synaptic transistor, and multi-gate synaptic transistors. Synaptic transistors with different working mechanisms can be applied in many scenarios, and also provide valuable reference for the development of a new generation of smart electronic devices.

2.2.1 The vertical synaptic transistors. Planar field effect transistors have made significant advances in neurosynaptic devices, but the development is limited by channel length, which makes it difficult to achieve high currents at low voltages. In contrast, vertical field effect transistors (VFETs) that differ in structure and operating mechanism could effectively compensate for the proposed deficiencies.[42,43] VFETs regulate channel length by adjusting the thickness of the active layer, allowing channel lengths to be simply controlled at the nano-meter level.[42] This means that VFET devices have superior on-current and can operate at low voltages, substantially reducing power consumption. In addition, since the electrodes in VFETs are placed vertically, high density integration can be achieved by stacking across the strips, which provides reliable guidance for flexible low-power electronic devices. Light response synaptic devices with a VFETs structure are proposed firstly (Fig. 3a)

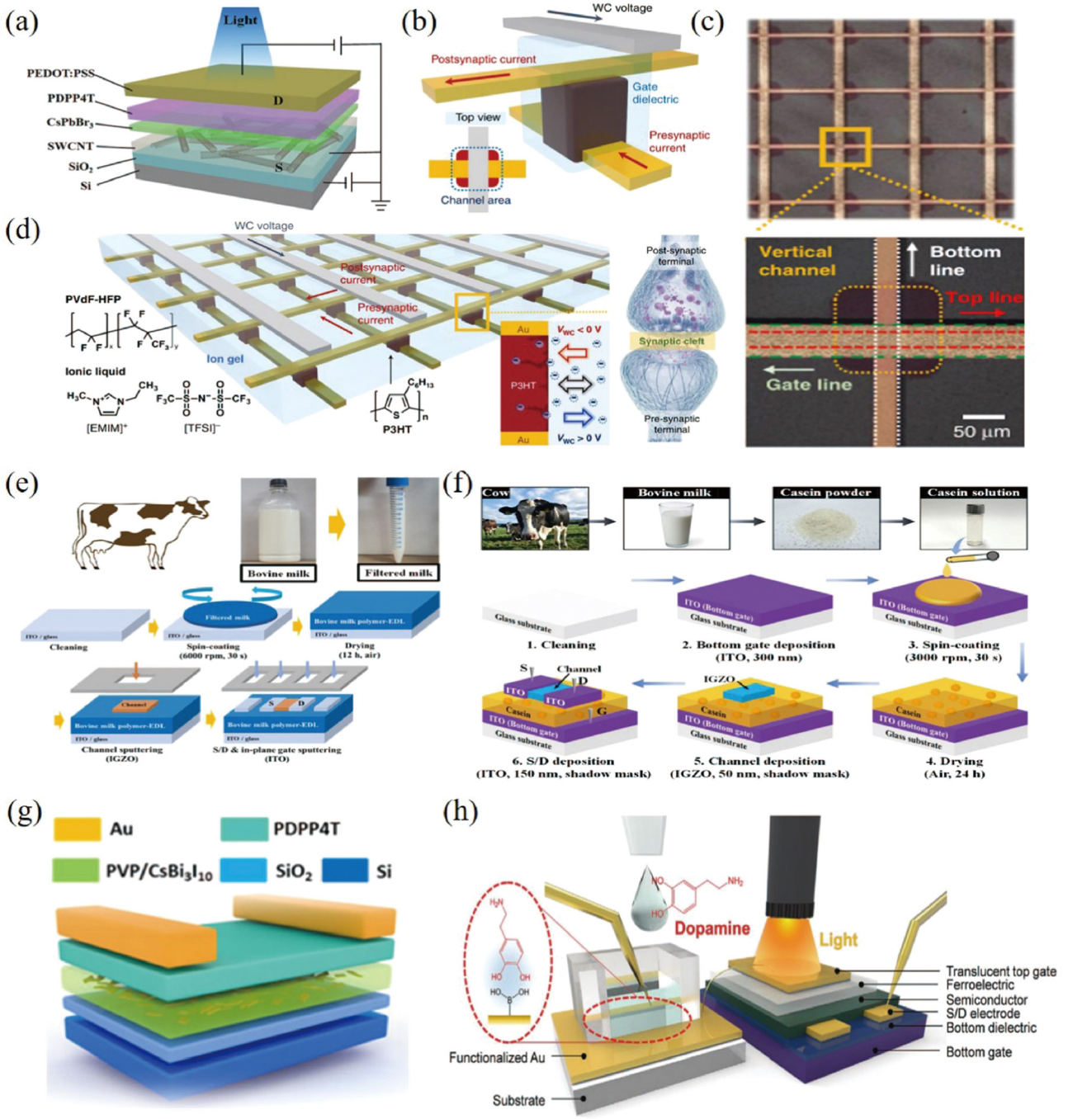

Fig. 3 Novel structural design of synaptic transistors. (a) Structure of vertical organic synaptic transistor (VOFET). Reproduced with permission.[43] Copyright 2021, Wiley-VCH. (b) Schematic diagram of a three-terminal synaptic device with a crossbar array structure. (c) Optical microscope image of a vertical crossbar synapse array. (d) Schematic diagram of an ion-gel gate modulated vertical crossbar synaptic array. Reproduced with permission.[75] Copyright 2020, Springer Nature. (e) Fabrication process of an organic electrical double layer synaptic transistor based on buttermilk polymer. Reproduced with permission.[90] Copyright 2022, Polymers. (f) Fabrication process of casein electrolytes for an organic electrical double layer synaptic transistor.[91] Copyright 2022, Nanomaterials. (g) Structural diagram of a floating-gate organic synaptic transistor based on lead-free calcium titanite material. Reproduced with permission.[92] Copyright 2021, American Chemical Society. (h) Extended gate organic synaptic transistor. Reproduced with permission.[93] Copyright 2021, Wiley-VCH.

through the combination of single-walled carbon nanotubes (SWCNTs) and poly[2,5-bis(2-octyldodecyl)pyrrolo[3,4*c*]pyrrole-(1,4(2*H*,5*H*)-dione-3,6-diyl)-*alt*-(2,2′; 5′, 2″; 5‴, 2‴′quaterthiophen-5,5‴-diyl)] (PDPP4T), PDPP4T provides charge trapping points, which result in a slower photocurrent decay process.[43] In addition, the minimum power consumption (only 1.3 fJ) is realized due to the inherent decreased channel of the VFETs and ultra-low operating voltage of 10 microvolts at the drain. To obtain high density

synaptic arrays, Choi *et al.*[75] proposed a vertical gate surround field-effect transistor (Fig. 3b) and three-dimensional crossbar synaptic array (Fig. 3c and d). The device exhibits different synaptic properties through the movement of ions in the ionic gel and a poly(3-hexylthiophene) (P3HT) vertical channel. In conclusion, thanks to the vertical structure, reduced channel length and symmetric conductivity state, high-density integration can be realized more quickly. Regrettably, vertical structure preparation requires more precise and meticulous process conditions. Therefore, the development of preparation processes for vertical synaptic transistors, such as printing technology, may be an effective process to reduce the preparation complexity for its additive manufacturing features.

2.2.2 The planar synaptic transistor. Different from vertical structure transistors, planar synaptic transistors are widely used by many researchers due to their simple and mature preparation process. Intelligent synaptic properties of the planar synaptic transistor induced by different mechanisms, including the electric double layer (EDL) effect, floating gate effect, electret effect, carrier capture and iron polarization effect *etc.* have also been widely studied, and synaptic transistors with the desired function can be constructed with single or multiple mechanisms in a synergistic manner. In this section, synaptic properties induced by EDL and floating gate mechanisms are emphasized, and their influence on synaptic properties is described in detail. Recently, several biocompatible and eco-friendly materials, such as starch, chitosan, and cellulose nanopaper have been used in planar artificial synaptic devices to form EDL structures. EDL transistors have large capacitances (>1 μF cm^{-2}), low drive voltages and thus low power consumptions. Kim *et al.* proposed a novel synaptic transistor using a natural cow's milk-based biocompatible polymer as an electrical double layer (Fig. 3e).[90] Due to the proton-induced EDL effect, the transistor shows a capacitance of up to 1.48 μF cm^{-2} at low frequencies (1 Hz). They prepared EDL synaptic transistors (Fig. 3f) using casein electrolytes rich in mobile protons and successfully simulated basic biological synaptic behaviour relying upon the EDL effect and achieved 90% recognition rate in handwritten MNIST learning simulations.[91] Thus, transistors with EDL materials could achieve artificial synaptic functions from a wide range of sources, which shows promising application prospects and provides a valuable reference for eco-friendly and biocompatible neuromorphic systems. However, it is worth noting that the stability of the synaptic transistors prepared by this structure needs to be further improved. Additionally, floating gate transistors are considered suitable devices for simulating synaptic behaviour because of their advantages in integrated circuit compatibility, large area processability, and multi-state storage. Metal halide perovskites (MHPs) are widely used to fabricate synaptic transistors due to their excellent light absorption capability and simple preparation process. Wang *et al.* reported a lead-free perovskite $CsBi_3I_{10}$ floating gate transistor (Fig. 3g) for optoelectronic synaptic devices.[92] The lead-free perovskite $CsBi_3I_{10}$/polyvinylpyrrolidone (PVP) was used as the photosensitive floating gate layer to trap charge, and the doping of PVP resulted in improved smoothness, enhanced photo responsiveness and photosensitivity. Due to the excellent photo-responsiveness of $CsBi_3I_{10}$ and the high charge mobility of PDPP4T, the device can exhibit a significant synaptic performance at an ultra-low voltage of -0.01 V, which provides a conceptual guide for subsequent construction of low-power synapses using floating-gate transistors. Unfortunately, the channel length and low conductance of planar synaptic transistors limit their use in high-speed synaptic electrons and high-density integrated synaptic electrons compared to vertical transistors. Therefore, more in-depth research needs to be invested in planar synaptic transistors to break through this limitation.

2.2.3 The extended gate synaptic transistor. In order to expand functions of synaptic transistors and optimize synaptic performance, the extended gate synapse transistors (they can be either vertical or planar structures) are constructed in a single device. For example, the muti-gate transistor can not only improve synaptic plasticity but also expand the signal sensing range including the introduction of chemical and biological signals. In this context, dual-gate organic synaptic transistors (DGOST) with a dopamine-responsive extended gate electrode are realized, which could avoid direct contact of the electrode and semiconductor with the buffer solution (Fig. 3h).[93] This design successfully simulates representative synaptic functions and reproduces the activity of real hippocampal neurons in a more efficient way. In addition, it can also significantly reduce device power consumption, detect extra dopamine signals and present the advantages of dual-gate synaptic transistor geometry. This functionalized extended gate electrode and hippocampal-synaptic transistor overcomes the limitations of previous artificial synaptic devices with a single function and provides an important reference for future multifunctional chemical sensing detection neural systems.

In summary, the development of different device structures and working mechanism can further control the synaptic properties at a more accurate level. For example, the vertical structure for low-power synapses, the planar structure with an EDL principle for degradable synapses, the floating-gate principle for non-volatile synapses, and the extended gate for multifunctional synapses. However, the complexity of the process, the stability of the performance, the improvement of cost, *etc.* also exist in different structures and principle. Therefore, it is necessary to find a balance in the future to achieve better foreground.

3. Multifunctional synaptic devices

The progression of optoelectronic synapses based on phase-change transistors,[100] floating-gate transistors,[46] ferroelectric transistors[101] and electrochemical transistors[102] have created new breakthroughs toward sophisticated artificial sensing systems analogous to that of humans. However, greater challenges remain in the construction of multifunctional synaptic device at the single device level. This subsection focuses on the review of multifunctional synaptic transistors with stretchable, degradable, multi-mode and reconfigurable functions at the

single device level. These features not only enrich the application scenarios of the devices but also alleviate the problems of electronic waste and the difficulty of integrating various functional devices with high density in the More than Moore era. Stretchable electronics are accelerating the integration of human-machine interface and Artificial Intelligence (AI) due to its excellent flexibility and tensile properties. In the beginning, stretchable materials, individual stretchable devices and stretchable electronic circuits were widely studied. Further to the post-Moore era, the advent of the physical limit and the limitation of the separation of storage and computation in the von Neumann architecture promoted booming-research on multifunctional stretchable synaptic electronics. Thus, the development from stretchable materials and individual devices to integrated circuits will be briefly traced. Stretchable individual synaptic devices, multiple arrays, and the integration and simulation of multifunctional synapses will be highlighted.

3.1. Stretchable devices

Humans and animals possess flexible and stretchable synapses that can adapt to all kinds of deformation. Similar to biological synapses, stretchable smart synaptic devices have broader applications such as skin health monitors, neuro-prosthetics and flexible robots.[103] Therefore, stretchable synaptic devices consisting of stretchable materials are expected to meet the needs of brain-like chips in various deformable situations. Except for intrinsically stretchable materials such as carbon nanotubes, silver nanowires, nanofiber networks, *etc.* most semiconductor materials have been implemented with molecular design and structural adjustments to improve stretchability. The advancement of strain tolerance is effective but the sacrifice of mobility occurs at the same time. To maintain the mobility during stretching, phase separation induced elasticity (Fig. 4a) is first introduced by employing poly(2,5-bis(2-octyldodecyl)3,6-di(thiophen-2-yl)diketopyrrolo[3,4-*c*]pyrrole1,4-dione-*alt*-thieno[3,2-*b*]thiophen) (DPPT-TT) as a high-mobility semiconducting polymer and polystyrene-*block*-poly(ethylene-ranbutylene)-*block*-polystyrene (SEBS) as the soft elastomer (Fig. 4b), and this work contributed to high-performance stretchable semiconductors for stretchable devices.[104] Two years later, highly stretchable organic transistors with high-mobility are produced (Fig. 4c) befitting from the high capacitance (5.5 μF cm^{-2}), outstanding transparency (Fig. 4d) and stretchability of ionic thermoplastic polyurethane (i-TPU).[105] In addition, Zhang *et al.* demonstrated a fully stretchable organic electrochemical transistor combining transfer patterning technology with a pre-stretched PDMS substrate to overcome the challenges of large-area patterning and integration techniques (Fig. 4e).[52] Recently, stretchable transistor arrays (347 transistors per square centi-meter) enabled skin electronics circuits were fully demonstrated (Fig. 4f).[106] Fig. 4g shows the array adheres to a human palm demonstrating a good fit between the skin and circuit. The integration of stretchable materials, stretchable device arrays, and stretchable skin circuits ultimately demonstrates superior performance and stability, laying the foundation for the next generation of more complex stretchable skin electronics. Through the above discussion, basic stretchable transistors have realized the development from performance to large area integration. However, multifunctional smart synaptic electronic systems have become the focus of research in recent years, expecting to overcome the traditional von Neumann bottleneck, and thus, the next section mainly focuses on the development of multifunctional synaptic devices.

Stretchable transistors used for synaptic electronics not only mimic excitatory and inhibitory functions similar to the nerves, but also assume paramount importance in the field of soft robots and neuromorphic systems. To date, stretchable transistors and synaptic responses have been successfully developed by using a single synaptic device or a combination of sensing systems. However, the diverse synaptic properties, the motion sensing controlled by synaptic devices, and the controllable multilevel storage states still face challenges due to the cognitive deficiency in materials, technologies, and physical mechanisms.[107–110] This subsection provides an overview from simple stretchable synaptic devices to complex multifunctional synapses. A low voltage stretchable synaptic was realized using scalable route inkjet-printed, which display mobilities as high as 30 $cm^2 V^{-1} s^{-1}$ and working voltages as low as 1 V, thanks to the double layer capacitive in poly (vinylidene fluoride-co-hexafluoropropylene) (PVDF-HFP) dielectric (Fig. 5a and b). Furthermore, the simple synaptic behaviour of neurons was imitated as shown in Fig. 5c.[8] In addition, based on the previous results shown in Fig. 4a, stretchable phototransistors are constructed with hybrid PDPP-TT and SEBS in a weight ratio of 5 : 5, which shows an outstanding photo-sensing performance even at a strain up to 100%.[111] Based on worm-like blended films, top-contact transistors were fabricated combining sequential thermal lamination with transfer procedures (Fig. 5d). Fig. 5e is the corresponding rapid and increased switching to X-ray pulse under different dose rates. Additionally, the device displayed outstanding optical transparency both in the original state and under strain up to 100% (Fig. 5f). The transistors were able to recover to the original state even experiencing stretching, twisting and pocking deformations (Fig. 5g). These devices were also sensitive to faint UV light, which is difficult to distinguish by human eyes (Fig. 5h). Furthermore, the combination of stretchable synaptic transistors and ANN simulation enables digital identification. The top-gated synaptic devices are fabricated using a stretchable bilayer semiconductor (Fig. 5i). Even at a 80 mV presynaptic pulse, the device also exhibits memory characteristics and thus low energy consumption. More noteworthy, when the transistors are stretched by 50%, the image recognition accuracy is still maintained at over 90% (Fig. 5j).[9]

With the advancement of research, more complex and versatile stretchable synaptic transistors have been successfully constructed as shown in Fig. 6. Lee *et al.*[51] reported the organic optoelectronic synapse system by recognizing and converting photoelectric signals into Morse code (Fig. 6b), and furthermore, artificial muscles were controlled through postsynaptic electrical responses (Fig. 6a). This work promotes the

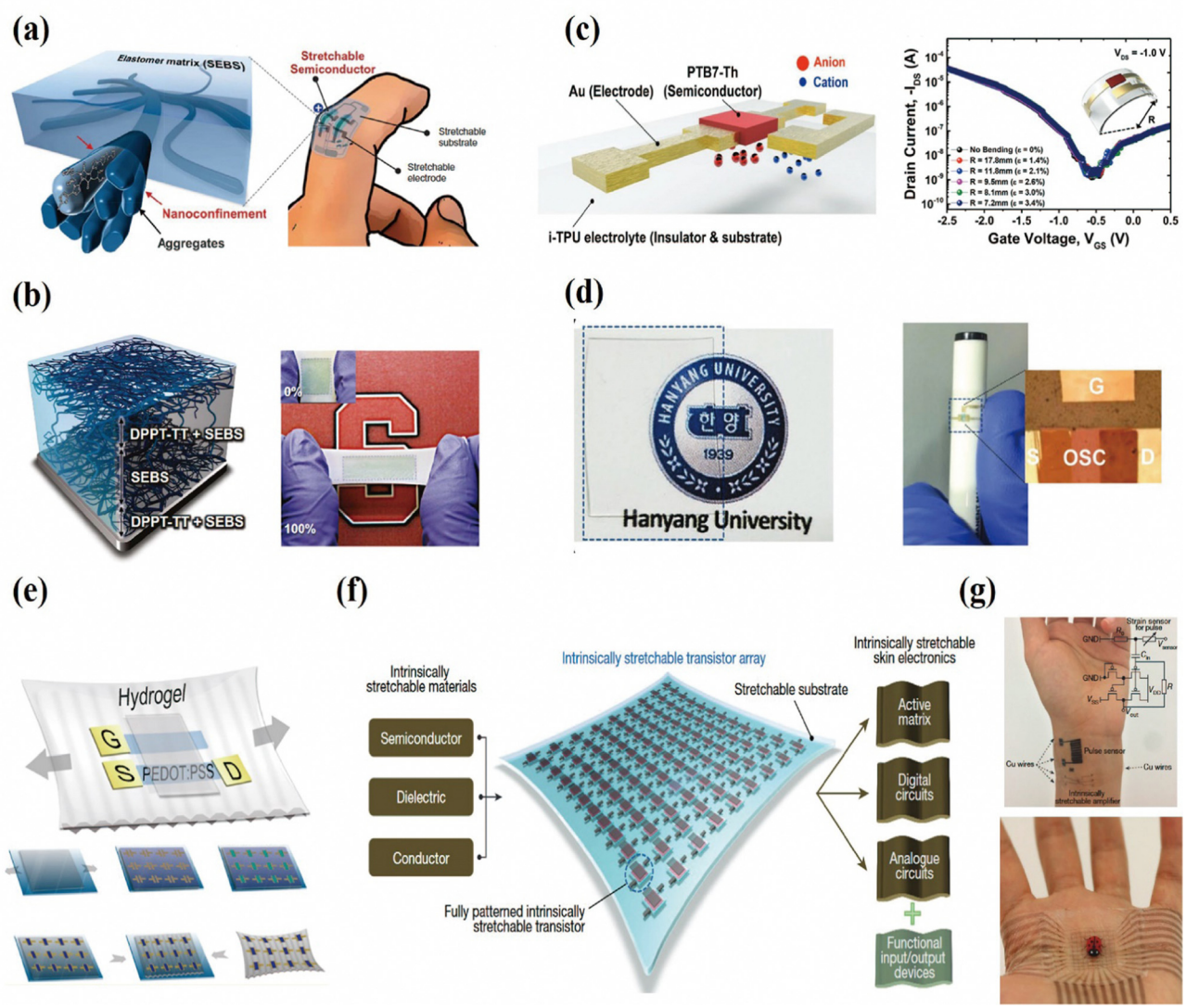

Fig. 4 Material design strategies for stretchable transistors. (a) Schematic of idea nanoscale networks of polymer semiconductors for the use of stretchable transistors. (b) A 3D illustration of the experiment nanoscale networks of polymer semiconductor. Reproduced with permission.[104] Copyright 2017, American Association for the Advancement of Science. (c) Schematic of i-TPU electrolyte-gated coplanar OFETs and transfer curves at different bending radii. (d) Photograph of a transparent i-TPU film and optical microscopy image of a coplanar-type organic transistor. Reproduced with permission.[105] Copyright 2019, Wiley-VCH. (e) Schematic of transferred OFETs arrays on a PDMS substrate.[52] Copyright 2017, American Chemical Society. (f) Diagram of an intrinsically stretchable transistor array. (g) Schematic of the array adheres and conforms to a human palm.[106] Copyright 2018, Nature.

development of bioinspired soft electronics and neurologically inspired robotics. In 2019, fully stretchable transistors and integrated synaptic systems were constructed with all rubbery based materials as shown in Fig. 6c, which shows no mechanical damage after stretching up to 50% with 1000 cycles.[76] Furthermore, the deformable synapse and corresponding synaptic transmission process is shown in Fig. 6d. Multifunctional intelligent synaptic function like the filtering behaviour of a synaptic transistor was further demonstrated (Fig. 6e). This work further combines the rubbery synaptic transistor and neurologically integrated system with multifunctions, which enrich neurological functions and pave the way toward soft machines. Multimode and multifunction electronic devices provide the possibility for a human–machine interface. Zhang *et al.*[112] proposed a stretchable multimodal neuromorphic array including situ temperature-responsive, strain-responsive and excellent self-healing functions (Fig. 6f), which is similar as human skin to sense, deliver and memory external environmental changes. In order to improve the mechanical deformation ability, P3HT nanofibers are used as semiconductors for stretchable organic synaptic transistors. After experiencing large stretching deformation, the synaptic transistors also exhibited excellent mechanical stability. The number of channel carriers and synaptic plasticity are further controlled by adjusting the ions in the ion-gel dielectric layer. Based on this, different decay constants and functionality are simulated

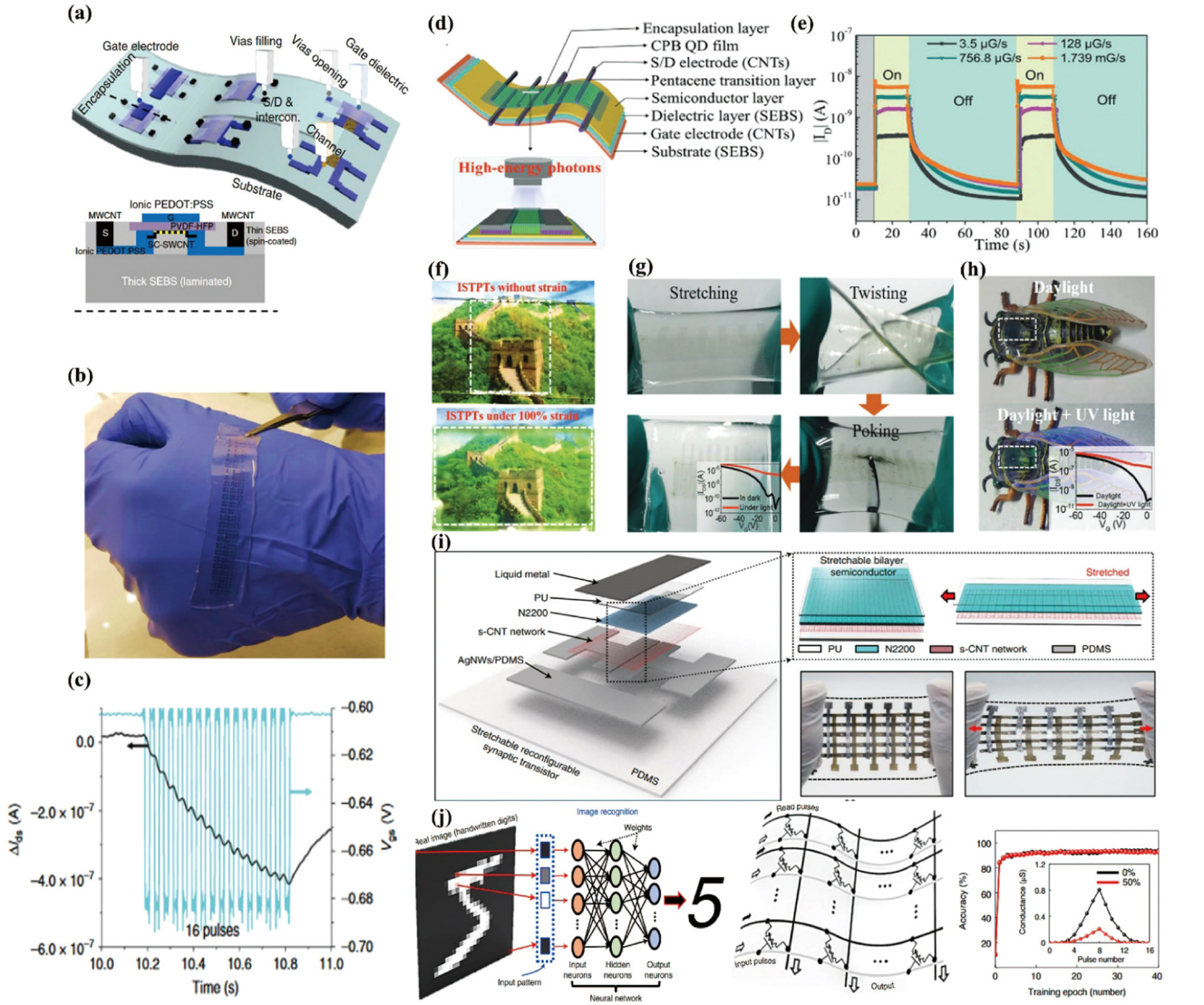

Fig. 5 Simple stretchable electronics. (a) Schematic of printed stretchable transistors. (b) Picture of a large area array of transistors and bent over a hand. (c) Typical postsynaptic current with 32 gate voltage pulses. Reproduced with permission.[8] Copyright 2019, Nature. (d) Schematic illustration of the device, worm-like CPB QD film as the photosensitizer. (e) Device response to X-ray pulse on and off under various dose rates. (f) The optical transparency of the device without strain and with 100% tensile strain. (g) Optical image of the device after stretching, twisting, pocking deformations, and finally recovery to the initial state. The inset displays the device characteristics after mechanical deformations. (h) The skin conformability of the device attached to a rubber cicada under daylight and daylight/UV light. Reproduced with permission.[111] Copyright 2022, Wiley-VCH. (i) Schematic of the synaptic transistor using bilayer semiconductors. (j) Schematic diagram of intelligent network image recognition, the deformable crossbar array and recognition rate curve. (i) and (j) were reproduced with permission.[9] Copyright 2022, Nature.

(Fig. 6g).[113] One year later, the vertical organic field effect transistor is constructed by the same group, which can effectively reduce the channel length, implement a high current density (5.19 mA cm^{-2}), and thus obtain a low working voltage (−0.5 V). Based on this, Guo *et al.*[114] coupled a triboelectric nanogenerator (TENG) and synaptic transistor, which ensures the direct interactions between external information and human machine interface (Fig. 6h). The evolution from the design of stretchable materials, stretchable transistors with simple synaptic functions to abundantly multifunctional stretchable synaptic transistors will undoubtedly promote the development of stretchable electrons in human brain computing. Therefore, the total stretchability of the material, the improvement of performance and its combination with the skin will further promote the development of stretchable synaptic transistors in the future.

3.2. Degradable devices

With the tremendous growth of electronic-waste (e-waste), biodegradable electronics have opened up great opportunities for green and sustainable neuromorphic electronics both in academia and industry. E-Waste not only pollutes the environment but also harms human health. Therefore, the development of green degradable materials and artificial synaptic

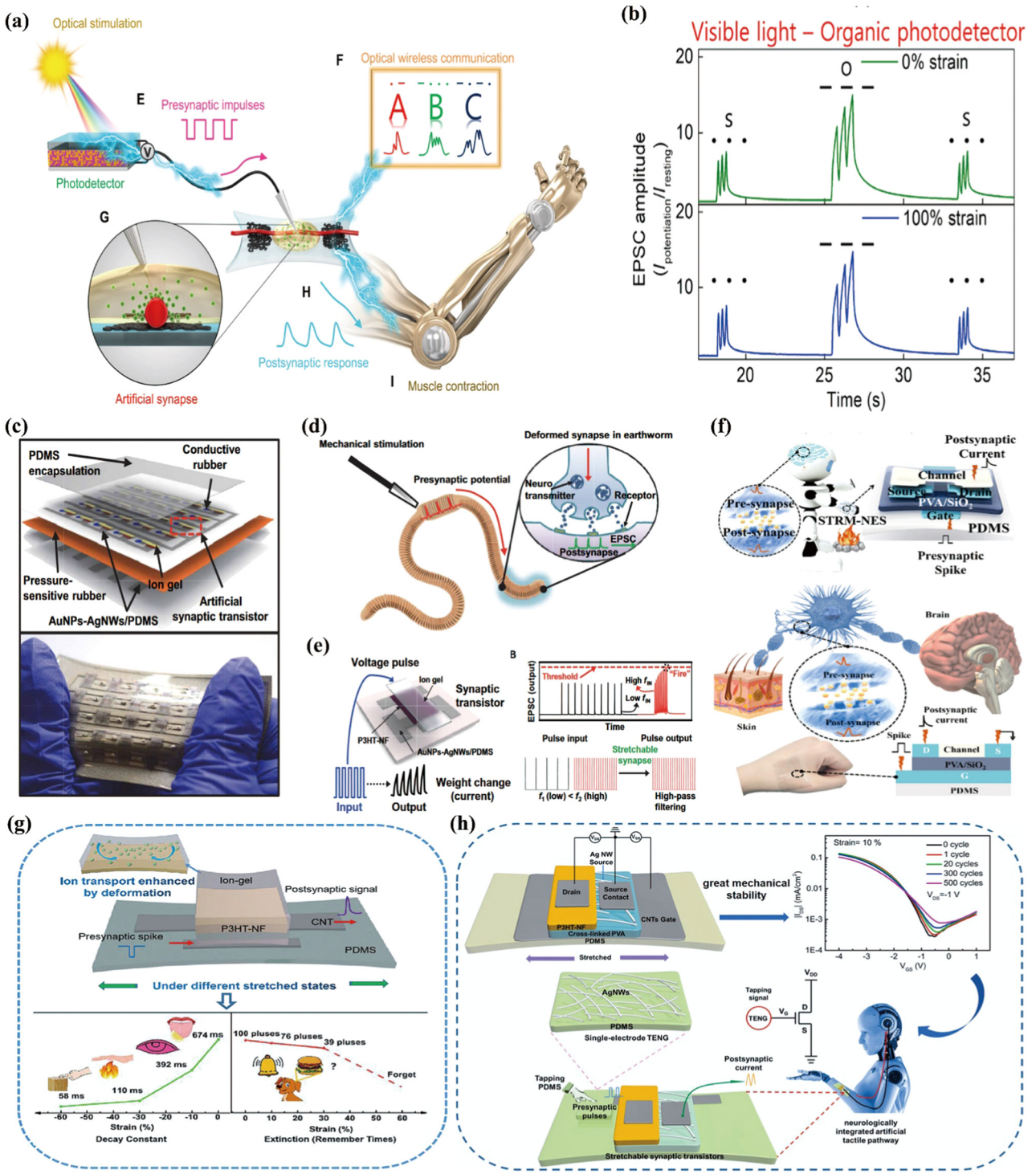

Fig. 6 More complex stretchable synaptic transistors. (a) Schematic of the generated action potential from light stimulates in an organic artificial system. Stimulus production, signal encoding, signal transfer, stimulus response, and muscle movement (E to I). (b) Visible light-triggered EPSC amplitudes of synaptic devices representing the international Morse code of "SOS". Reproduced with permission.[51] Copyright 2018, American Association for the Advancement of Science. (c) Schematic of the integrated tactile sensory system. (d) Illustration of the synaptic transmission in a deformable synapse. (e) Schematic of synaptic transistor responses to multiple presynaptic pulses and illustration of high-pass filtering behaviour. Reproduced with permission.[76] Copyright 2019, American Association for the Advancement of Science. (f) Schematic illustration of a multimodal temperature-responsive synaptic transmission process through different stimulation signals. Reproduced with permission.[112] Copyright 2022, American Chemical Society. (g) Schematic illustration of stretchable organic synaptic transistor based on P3HT nanofiber semiconductors. Reproduced with permission.[113] Copyright 2020, Elsevier. (h) The coupling of a vertical organic field effect transistor and triboelectric nanogenerator (TENG) used in human-machine interfacing. Reproduced with permission.[114] Copyright 2021, Elsevier.

devices is expected to reduce the harmful effects of e-waste on the environment and humans, and promote the development of green brain-like chips. Furthermore, degradable synaptic transistors also open the doors for ''green'' brain-computer interfaces and flexible artificial intelligence systems.[115] In 2020, Huang *et al.*[60] first introduced natural chlorophyll into organic semiconductors to build a multifunctional organic transistor, which can achieve both photodetection and synaptic functions by controlling the gate voltage (Fig. 7a). The introduction of natural chlorophyll offers the possibility for degradable synaptic transistors, however, the degradability of the devices was not further explored as it was constructed on rigid substrates. One year later, the group further compounded chlorophyll-*a* and carbon nanotubes to construct degradable photonic synaptic transistors shown in Fig. 7b.[115] Furthermore, low energy consumption (17.5 fJ per pulse) was realized at a low drain voltage of −0.0001 V. Fig. 7c demonstrates the environmentally friendly properties of the transistor array with good degradability, which provides the possibility to next-generation degradable neuromorphic electronics. Liu *et al.*[97] constructed biodegradable organic synaptic transistors (Fig. 7d) using natural neutral polysaccharides from dextran (Fig. 7e) as dielectrics for the proton conduction properties. A glutaraldehyde (GA) crosslinking method was introduced to control the hydroxyl contents and proton conduction, and Fig. 7f shows the reaction principle. The synaptic devices adhered to an uneven brain model indicating the ultra-flexibility and promising potential in future wearable electronics (Fig. 7g). The array of devices shown in Fig. 7h disappeared within 15 seconds of dripping, indicating excellent degradability. Degradable and ultra-flexible synaptic transistors were designed using natural apple pectin as the dielectric.[116] Due to the proton-induced electric double layer and thus the high capacitance of pectin, the operating voltage of a single synaptic was reduced to −20 mV as shown in Fig. 7i. Furthermore, it can be degraded in water within 100s after it completes its function, which provides a powerful opportunity to create ''green'' biological neuromorphic systems. More strikingly, both ultra-flexible and degradable self-supporting organic synaptic transistors for neuromorphic applications are achieved based on natural polysaccharide dielectrics.[59] The resulting device is as thin as 309 nano-meters, so possesses excellent flexibility and degradability as shown in Fig. 7j. Fig. 7k displays outstanding conformability while adhering to a human brain model and can be degraded in water without any toxic by-products. The above research demonstrates the potential of green sustainable electrons towards artificial neural networks, from the degradability of monolayer materials to the acquisition of self-supporting devices and ultra-flexible degradable properties. However, it still faces challenges from partial degradation to complete degradation.

3.3. Multimodal and reconfigurable devices

The ubiquity of information technology leads to the generation of a large amount of data. Especially in the era of data explosion, there is a high demand for multifunctional, multi-mode transistor devices, which have greater storage capacity, information processing capacity, and therefore exhibit more diverse neuronal functionalities. A reconfigurable single-gate artificial synaptic is constructed employing hydrogen-rich silicon nitride film and ambipolar graphene as the gate dielectric and semiconductor, respectively.[117] The dynamic reconfigurable synaptic functions are attributed to the ambipolar property of graphene, two kinds of hysteresis induced by the traps and ions in SiNx:H film. Based on this, more complex functions like the modulation of tactile perception have been imitated shown in Fig. 8a. Higher voltages (15 V/−15 V) induce ion movement and modulate operating modes of transistors (excitatory or inhibitory). Smaller gate voltages (5 V/−5 V) induce trapping of holes and electrons, which in turn modulates the channel conductance to achieve different responses to the same gate voltage stimulus. The gate voltage stimulation (5 V/−5 V) represents two states (heat and cold, Fig. 8a-1). When a transistor is in the excitatory mode (Fig. 8a-2), the positive signal (heat stimulus) results in a potentiation behaviour (''Ah, it's not okay!''). The negative signal (cold stimulus) results in a depression behaviour (''Well, it's okay!''). However, if the synapse is set to the inhibitory mode (Fig. 8a-3), the positive signal (heat stimulus) causes depression behaviour. The negative signal (cold stimulus) induces a depression behaviour. Since the charge trapping and polarization show opposite effects on the channel conductance,[118–121] Wang *et al.*[77] further utilized electret trapping combination with an electrochemical induction composite dielectric layer to construct an electrochemical-electret coupled organic synapse with reconfigurable facilitation-to-depression switching capabilities under the same presynaptic gating pulses. Fig. 8b is the stacked structure of an organic synapse including tri-layer dielectric, poly(vinylidene fluoride-trifluoroethylene-chlorofluoroethylene) terpolymer [P(VDF-TrFE-CFE)] served as a dielectric to reduce operation voltages, poly(2-vinylnaphthalene) (PVN) served as electret to trap charge, poly[(1-vinylpyrrolidone)-*co*-(2-ethyldimethylammonioethyl methacrylate ethyl sulfate)] [P(VP-EDMAEMAES)] served as a buffer protective layer and poly(isoindigo-*co*-bithiophene) (PIID-BT) was used as the channel material. Under a low gate voltage pulse, electrochemical doping dominated the channel conductance, which induced synaptic facilitation, and conversely, when increasing voltage pulse, electret charging is triggered which induced synaptic depression due to the depletion of charges (Fig. 8c).

In addition to controlling channel conductance through charge trapping and induction, bipolar semiconductor materials can operate in different modes to induce reconfigurable synaptic properties. Wei *et al.*[122] utilized ambipolar conjugated-polymer poly[2,5-bis(2-decyltetradecyl)pyrrolo[3,4-*c*]pyrrole-1,4(2*H*,5*H*)-dione-*alt*-5,5′-di(thiophen-2-yl)-2,2′-(*E*)-1,2-bis(3,4-difluorothien-2-yl)ethene] (PDPP-4FTVT) as a semiconductor constructed reconfigurable intelligent synaptic device (Fig. 8d). The device can respond oppositely to the same gate voltage stimulus signal, which is achieved by changing the operating mode of the ambipolar transistor (Fig. 8e and f, initial and programmed state). When the device is operating in the original state (electron transport), electrons are injected into the insulator layer under positive gate pulses, which result in the decreased PSC (Fig. 8g),

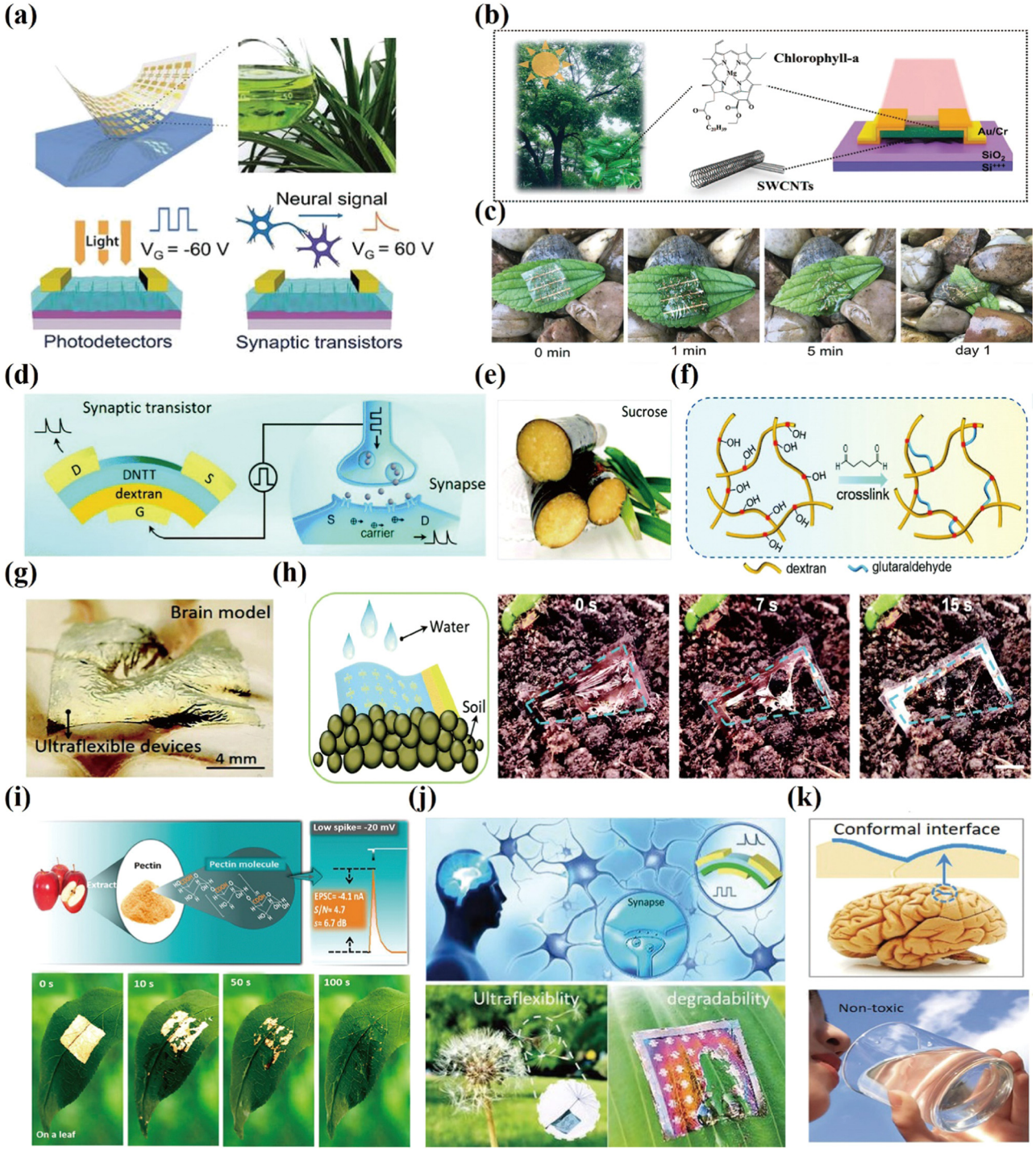

Fig. 7 Degradable synaptic transistors. (a) Structure of photodetectors and a synaptic transistor based on natural Chlorophyll/Organic Semiconductors. Reproduced with permission.[60] Copyright 2020, Wiley-VCH. (b) Schematic of the chlorophyll-*a*/SWCNTs synaptic transistor. (c) The degradable process of the chlorophyll-*a*/SWCNTs composite transistor array. Reproduced with permission.[115] Copyright 2021, Wiley-VCH. (d) Schematic of an artificial synaptic transistor (left) and biological synapse (right). (e) The sources of dextran. (f) The changes of hydroxyl content before and after crosslinking. (g) Synaptic devices adhered to a brain model. (h) Degradation process of the synaptic devices in water. Reproduced with permission.[97] Copyright 2020, Royal Society of Chemistry. (i) Degradation property. Reproduced with permission.[116] Copyright 2022, American Chemical Society. (j) Schematic illustration of the relationship between biological synapses and intelligent synapses, degradability and ultra-flexibility of transistor devices. (k) Non-toxicity and edibility of dextran, conformability to the human brain model using an ultrathin synaptic transistor. Reproduced with permission.[59] Copyright 2020, Wiley-VCH.

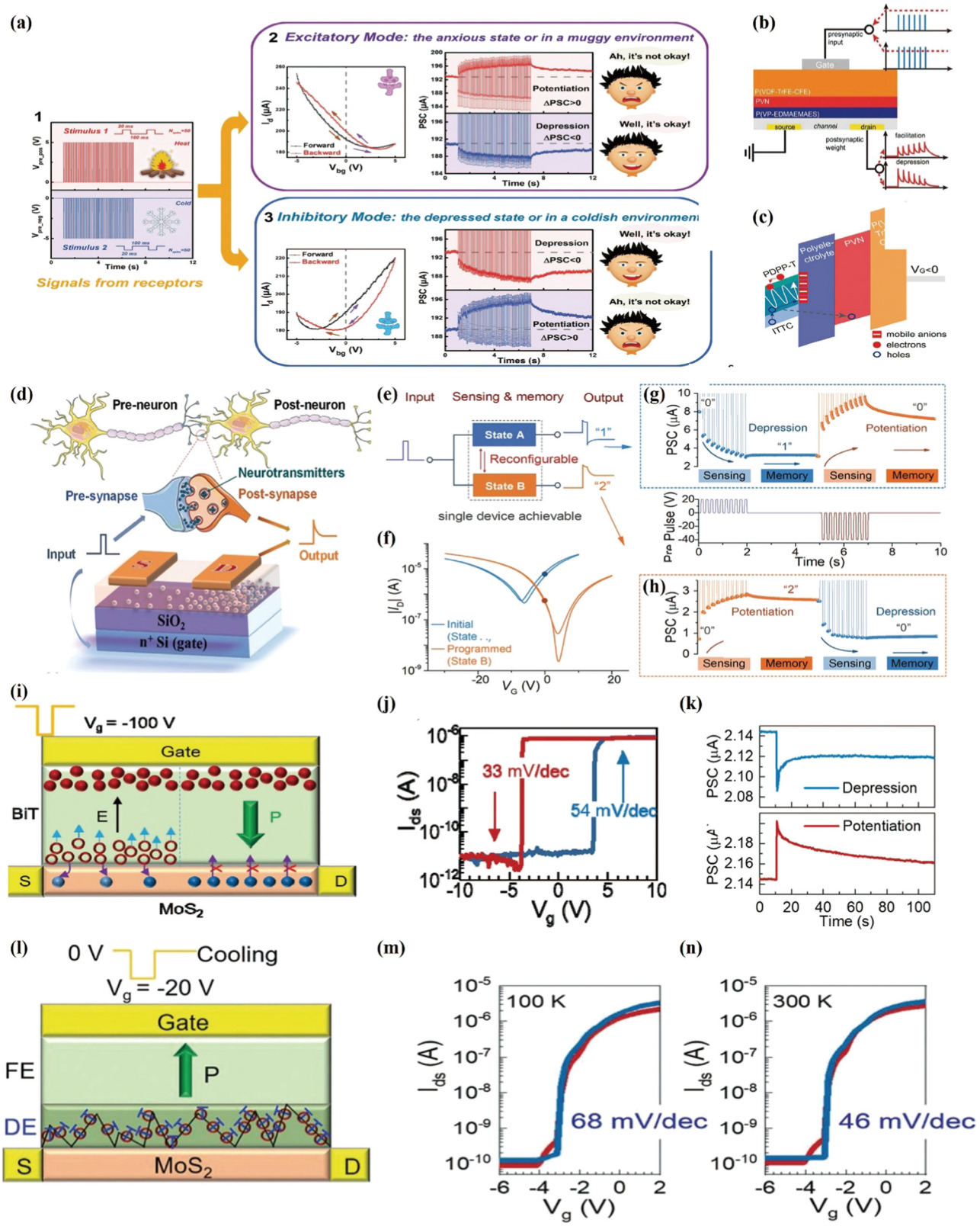

Fig. 8 Single-device based reconfigurable synaptic transistors. (a) Reconfigurable functions implemented by bipolar transistors. Reproduced with permission.[117] Copyright 2019, Wiley-VCH. (b) Device stacked structure as a neuromorphic device. (c) Working principle of electret capture and ion-induced modulation of the channel conductance. Reproduced with permission.[77] Copyright 2022, Wiley-VCH. (d) Schematic illustration of the ambipolar transistor for an artificial synapse. (e) Schematic and (f) transfer curves of the initial and programmed transistor. Different PSC responses of the (g) initial and (h) programmed ambipolar synapses to the same gate pulse. Reproduced with permission.[122] Copyright 2021, Wiley-VCH. (i) Schematic illustration of oxygen vacancies redistribution in BiT during (left) and after (right) the negative gate pulse. (j) Hysteresis loop of the transistor after the high negative gate pulse with SS $<$ 60 mV dec^{-1}. (k) Depression and potentiation behaviours of the transistor under gate pulses of −10 and 10 V, respectively. (l) Schematic illustration of pinning ferroelectric domain walls with Vo^{2+} after bias cooling. (m and n) Hysteresis-free transfer curves and subthreshold swing at 100 and 300 K, respectively. Reproduced with permission.[123] Copyright 2022, Wiley-VCH.

but increased PSC are acquired for the programmed transistor (hole transport) under the same positive gate pulses (Fig. 8h). Reconfigurable transistor and multi-mode memory functions are demonstrated by regulating ferroelectric oxygen vacancies distribution dynamics.[123] Fig. 8i shows the redistribution process of oxygen vacancies in $Bi_4Ti_3O_{12}$ during the negative gate pulse of −100 V, which results in a typical ferroelectric counter-clockwise hysteresis loop and low SS (54 and 34 mV dec^{-1} in forward and backward sweeps, Fig. 8j). Fig. 8k shows the corresponding synaptic excitatory (−10 V, 300 ms) and inhibitory properties (+10 V, 300 ms). More strikingly, a hysteresis-free logic transistor is realized possessing a subthreshold swing from 68 down to 46 mV dec^{-1} (Fig. 8m and n) by modulating the location of oxygen vacancies and pinning the ferroelectric domains through cooling control, as shown in Fig. 8l. These new proof of concepts of functional reconfiguration and muti-operation mode in a single-gate field-effect transistor is of great advantage in future multi-functional synaptic system applications.

4. Integration of artificial nervous systems

Giving the artificial nervous system the ability to sense the environment further enhances our ability to perceive the world. In addition, the use of a neural network system to control robot actions (The Artificial Sensorimotor Systems), the construction of the visual system and tactile system enabled by synaptic devices will further accelerate the realization of artificial intelligence. This section highlights the recent progress in this area and summarizes the future directions and challenges.

4.1. Artificial sensorimotor systems

Different spatiotemporal action potentials produced by an external pulse will be processed and identified through biological neural systems and finally transmitted to the human brain with low power consumption. An imitation human neural network based on biological synapses has become the key technique in bio-inspired electronics, which can effectively promote the development of human-computer interaction and intelligent robots. As shown in Fig. 9a, Kwon *et al.*[65] in real time according to the mechanisms of the biological semicircular canals by combining synaptic transistors with triboelectric rotation sensors. Rotational movement will trigger TENG rotation and generate voltage pulses to artificial synaptic transistors, which will be detected as different postsynaptic currents (Fig. 9b). This artificial nervous system is enhancing the prospects in neurorobotics and soft electronics across time and space. In living systems, the production of sensation and the domination of movement are dynamically linked and mutually reinforced. The real time communication between analog world information and robotic platforms could be realized through neuronal computation. Recently, processing and learning the target task with neuromorphic circuit is realized. The robot can navigate itself in a two-dimensional maze following a planned path after being trained with sensorimotor systems and organic neuromorphic circuits. However, the untrained robot is disoriented and cannot get out of the maze (Fig. 9c).[69] This demonstration paves the way for a sophisticated systems connection like rapid prototyping of intelligent and real-world systems. Moreover, Chen *et al.*[124] further combined a visual with a vestibule system to construct the artificial motion sensory system, in which TENG as a vestibule for sensing rotation and a synaptic transistor array as the retina are used. The human vision-vestibule integrated nervous system and artificial motion multisensory system are demonstrated in the left and right sight of Fig. 9d, respectively. The TENG and 1-TDA-$CsPbBr_3$ QDs in indacenodithiophene–benzothiadiazole (IDTBT) are used to simulate the rotation signal of the vestibule and receive the external optical signal, respectively. All these signals are eventually converted into electronic visual signals and electronic motion signals through synaptic transistors. These works provide a direction for development in multisensory integration, information processing, robot motion monitoring and artificial prosthetics.

4.2. The artificial visual system

The retina, as a light-sensitive layer, mainly transforms and memorizes light information and then adjusts brain activity. To date, many studies on optoelectronic synapses have been widely studied for their low crosstalk and high interference immunity, such as the imitating of colored and color-mixed pattern recognition of the vision system with a h-BN/WSe_2 heterostructure optic-neural synaptic device (Fig. 10a). This research demonstrates the stable conduction states (less than 1% variation), which accelerated the integration pace between neural networks and complex pattern recognition.[67] In addition, Zhang's group developed bionic optoelectronics based on OFETs with ultralow energy consumption of 0.07–34 fJ per spike by adjusting the source Schottky barrier and charge-carrier injection. Furthermore, flexible 8 × 8 OFET arrays for the artificial optic-neural network indicating excellent image recognition and contrast reinforcement abilities. The image recognition function was examined not only on a flat but also on a human eyeball mode with a bending radius of 11 mm (Fig. 10b). As the number of stimuli increases, the photocurrent weight also increases, and the image contrast enhancement function is realized, which demonstrates the potential for future applications such as to help blind people to regain their optesthesia.[125] In another example, Shen *et al.*[126] developed flexible artificial optoelectronic synapses (10 × 10 array, Fig. 10c) based on lead-free metal halide nanocrystals for neuromorphic computing and color recognition. The EPSC image mapping of the 10 × 10 array under 2, 20, and 40 s light duration proves enhanced visual perception function with a longer duration time (Fig. 10d). Moreover, the development of infrared artificial synaptic devices is conducive to night monitoring. Liu *et al.*[79] designed organic/inorganic hybrid heterojunction synaptic phototransistors for short-wave infrared night visual systems because the heterojunction structure can promote photogenerated exciton separation (Fig. 10e). As shown in Fig. 10f, the measured EPSC values and

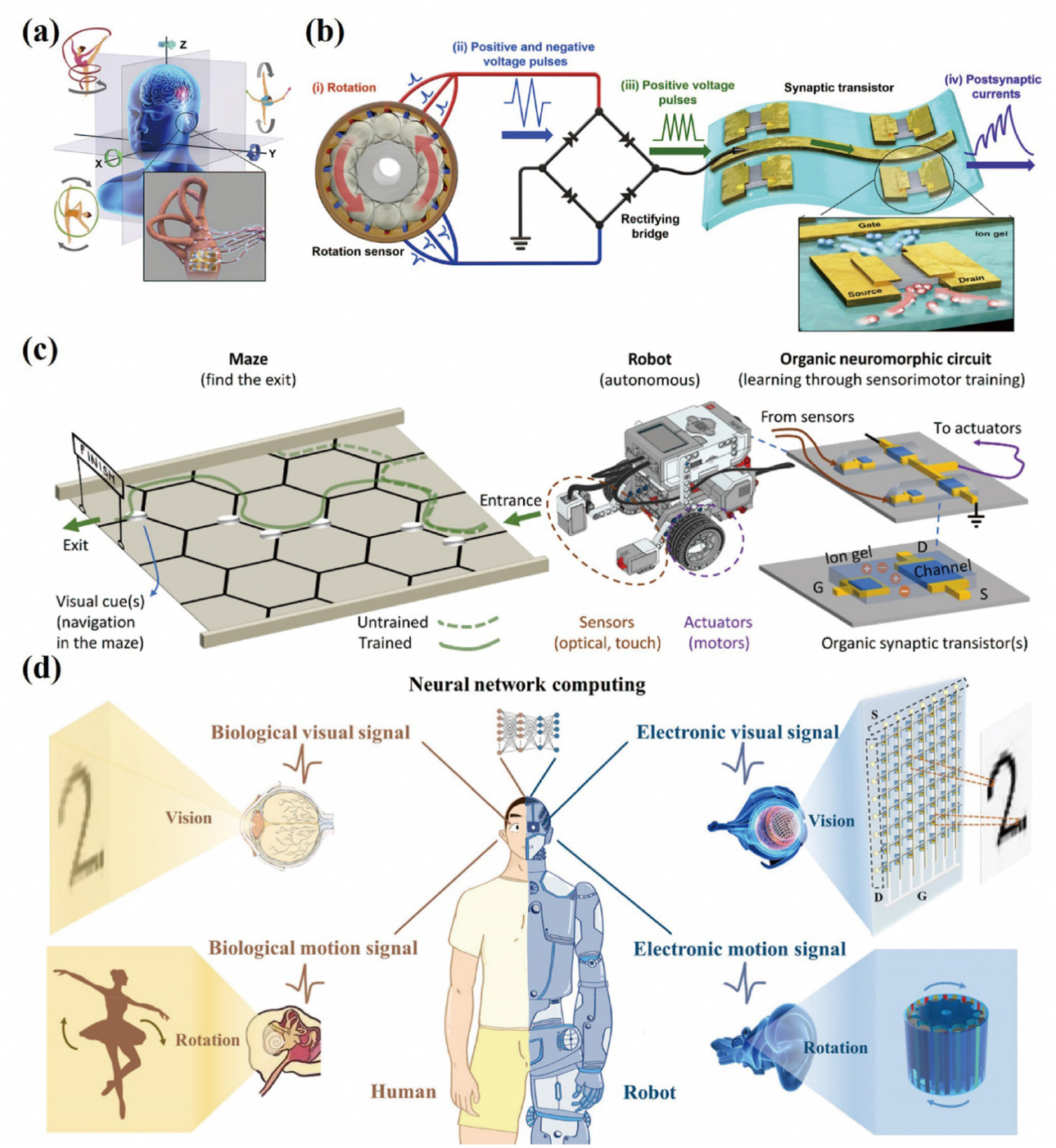

Fig. 9 Information processing system with robots. (a) Schematic diagram of the rotation detection based on the nervous system. (b) The artificial vestibular system and mechanism including a rotation sensor, rectifying bridge circuit, and synaptic transistors. Reproduced with permission.[65] Copyright 2020, Elsevier. (c) An autonomous robot gradually learns to navigate in a maze and finally found the exit. Reproduced with permission.[69] Copyright 2021, American Association for the Advancement of Science. (d) Schematic diagram of human vision and vestibule (left part), and an artificial motion sensory system (right part). TENG and transistor array act as the rotation receptor and retina for visual reception. Reproduced with permission.[124] Copyright 2022, American Chemical Society.

corresponding shape of "SIR" through a mask clearly appeared after 1100 nm SIR light even under a dark night, 200 and 500 cd m^{-2} white back-ground light night. This provides the direction for the artificial night vision. Furthermore, Liu *et al.*[127] constructed hemispherical biomimetic eyes using ultra-flexible and ultrasensitive near-infrared organic phototransistors, which are more suitable for integration with bioelectronic skin. The imaging system of the ultra-flexible

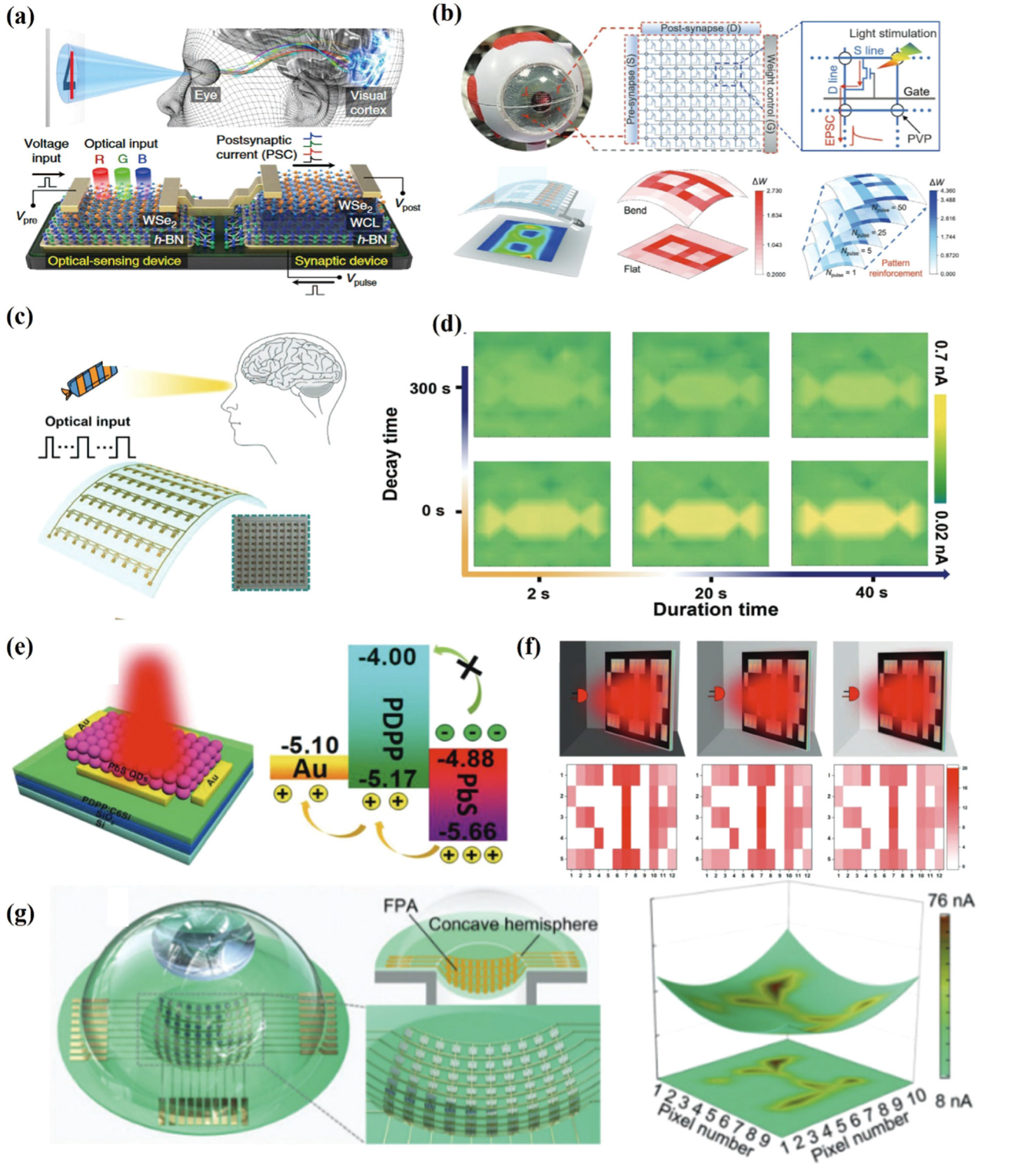

Fig. 10 Visual synaptic system. (a) Schematic of the optic nerve system and h-BN/WSe_2 synaptic device integrated with a h-BN/WSe_2 photodetector. Reproduced with permission.[67] Copyright 2018, Nature. (b) Schematic of the image recognition and reinforcement learning under flat and bending on a human eye-model. Reproduced with permission.[125] Copyright 2022, Wiley-VCH. (c) Schematic diagram of a human vision system and the flexible device. (d) The EPSC image mapping of the 10 × 10 array under 2, 20, and 40 s light duration. Reproduced with permission.[126] Copyright 2022, Wiley-VCH. (e) Structure and energy level diagram of synaptic transistors. (f) Measured EPSC values and corresponding shape of "SIR" through 1100 nm SIR light under the dark night, 200 and 500 cd m^{-2} white back-ground light night. Reproduced with permission.[79] Copyright 2022, Wiley-VCH. (g) Hemispherical biomimetic eyes enabled by an ultra-flexible array with a plano-convex lens integrated on the top and the constructed image (letter "H") of biomimetic eyes with 90 devices. Reproduced with permission.[127] Copyright 2022, Wiley-VCH.

hemispherical bio-mimetic eyes is shown in Fig. 10g, compared with planar image arrays, the letter "H" pattern shows higher contrast compared with flat plan for a more consistent distance. Therefore, it can be used as higher-resolution image systems. These works especially the ultra-flexible NIR imaging system will expand the further application of NIR visualization in biomedicine, visual prosthetics and intelligent bioimaging systems.

4.3. The artificial tactile system

Effective tactile information processing and recognition by a synapse transistor system allows for the integration of environmental signals and human skin systems. The recognition and transfer of strain signals mainly originated from the following working mechanisms including resistive, piezoelectric, and triboelectric-capacitive coupling response, which will be discussed separately in chronological order. The development of milestone artificial tactile systems in the most recent five years are introduced in Fig. 11. In 2018, Bao *et al.*[128] constructed an artificial tactile system by connecting resistive pressure sensors, organic ring oscillators (convert resistance signal into voltage), and a synaptic transistor (Fig. 11a). The as-prepared system could detect the movement of an object, combine simultaneous pressure inputs, and distinguish braille characters. Furthermore, a monosynaptic reflex arc can be executed from postsynaptic currents induced by voltage stimulation converted from a ring oscillator. In the same year, Chen *et al.*[129] converts pressure stimuli into electric signals through the pressure sensor, which is coupled into a synaptic transistor to record information (Fig. 11b). In addition to transforming the pressure signal by means of a resistance sensor, the nanogenerator can convert the pressure signal into a discontinuous electrical signal. As shown in Fig. 11c, a stretchable neurologically integrated robot was created combining TENGs and synaptic transistors. The action potentials from TENGs are transmitted into artificial synapse counterparts to execute memory functions.[76] In addition, a self-powered synapse transistor enabled by touching TENG to imitate synaptic functions without any additional voltage to generate pre-synapse spikes are realized. Moreover, the "AND" and "OR" logic functions were achieved and mimicked, which shows the great potentials in the applications of e-skin and human-computer interaction (Fig. 11d).[130] Flexible neurological electronic skin is developed combining a ferro-electret FENG and artificial synapse transistor. The tactile signal of force is converted by the FENG sensor, and then applied to the synaptic transistor gate for different postsynaptic currents and next stage transform (Fig. 11e).[131] Flexible strain organic synaptic systems controlled by capacitive

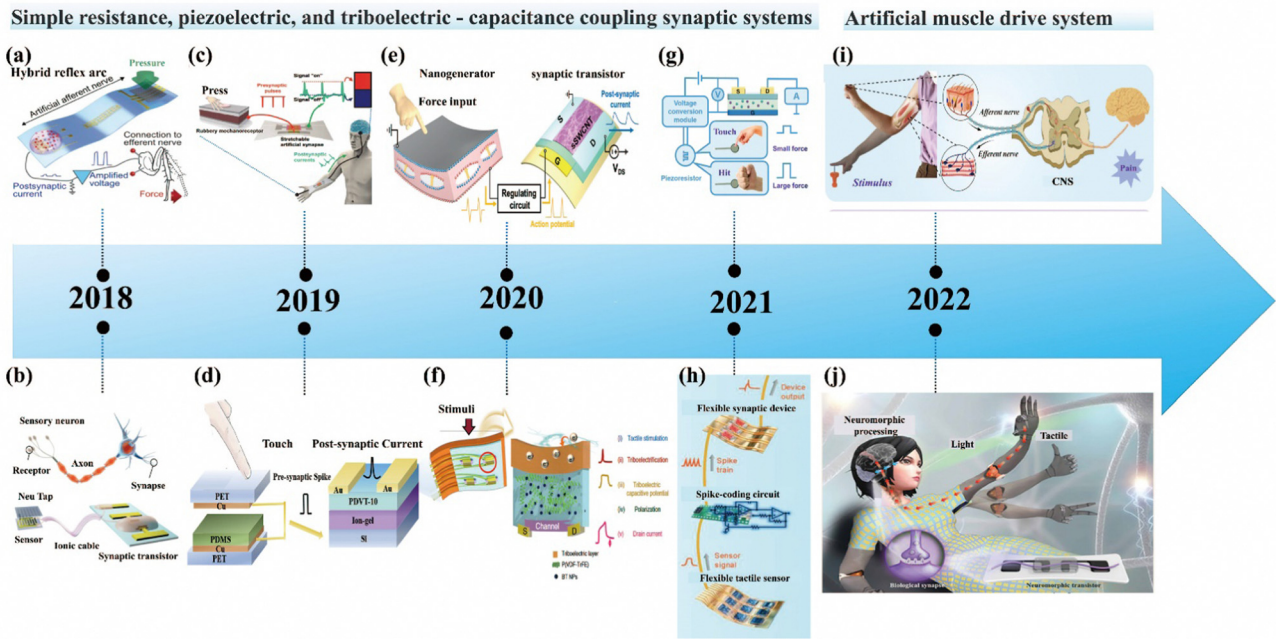

Fig. 11 The artificial tactile system in the recent five years. (a) The artificial afferent nerve composed of pressure sensors, ring oscillator, and synaptic transistor. Reproduced with permission.[128] Copyright 2018, American Association for the Advancement of Science. (b) The artificial afferent nerve including pressure sensors and synaptic transistors. Reproduced with permission.[129] Copyright 2018, Wiley-VCH. (c) Schematic illustration of a biological somatic sensory system with mechanoreceptor and synapse skin. Reproduced with permission.[76] Copyright 2019, Wiley-VCH. (d) Self-powered synapse achieved by touching TENG to produce a pre-synaptic spike. Reproduced with permission.[130] Copyright 2019, Elsevier. (e) Integration of ferro-electret FENG and an artificial synapse transistor. Reproduced with permission.[131] Copyright 2020, American Chemical Society. (f) Modulated drain current synaptic properties with aligned dipoles in the BT NPs/P(VDF-TrFE) nanocomposite by the generated triboelectric capacitive potential. Reproduced with permission.[132] Copyright 2020, Nature. (g) Schematic diagram of the tactile sensor circuit. Reproduced with permission.[133] Copyright 2021, Royal Society of Chemistry. (h) Schematic illustration of the flexible tactile sensory system. Reproduced with permission.[68] Copyright 2021, Elsevier. (i) Schematic illustration of an artificial somatosensory system. Reproduced with permission.[134] Copyright 2022, Nature. (j) Schematic illustration of gesture recognition. Reproduced with permission.[78] Copyright 2022, American Chemical Society.

coupling under touch are reported (Fig. 11f). By controlling the barium titanate nanocomposite composition in a ferroelectric poly(vinylidene fluoride-trifluoroethylene) dielectric to obtain memory functions.[132] Fig. 11g and h are both strain synaptic systems based on resistive sensors, except for the same signal transition principle, both works use induced coupling of ions in the dielectric layer to achieve synaptic function, which provides promising potential in artificial intelligence.[68,133] An artificial somatosensory system was developed utilizing multiple tactile sensor arrays, synaptic transistors and artificial muscles. Multiple sensors and multi-gate synaptic transistors are good for spatio-temporal information-processing. In addition, an artificial muscle could be moved by an instant feedback function (Fig. 11i).[134] Xu *et al.* further integrated the stress sensing signals of different gestures with intelligent synaptic transistors (Fig. 11j), and trained the artificial intelligence networks with different drain currents corresponding to different gestures, finally recognizing gestures with high recognition accuracy.[78] This work is an important step toward wearable intelligent human–machine interfaces.

5. Conclusions and perspectives

In conclusion, the relationships between the specific structural design of semiconductor materials, devices and synaptic properties are reviewed. Furthermore, synaptic applications based on transistors in stretchable, biodegradable, multi-modal reconfigurable, robotic information processing, vision system and strain perception are systematically summarized. Based on this, it is found that the emerging synaptic devices and integrated systems would be a new breakthrough in brain-like chips and even the realization of robotic connection. More strictly, giving more complex functions to individual synaptic devices such as stretchability, degradability, reconfigurability, and developing high-density synaptic systems to further mimic human activity will further advance the connection between intelligent and biological synapses. For example, the introduction of fully degradable synaptic devices to simulate reflexes in animals, the combination of electret and electrochemical materials to achieve multimodal, reconfigurable devices based on single synaptic transistors, organic polymer-based stretchable synaptic electronic systems, and photosensitive vision systems and self-powered strain interconnection systems will be an important way to accelerate the development of multifunctional synaptic electrons. In addition, printing technology is not only convenient and low cost but it is also easier to achieve a high throughput output. Therefore, novel materials and device structures, multifunctional synaptic devices, diversity of synaptic properties and synaptic sensing interconnection systems combined with high-throughput printing processes are expected to achieve multi-mode, intelligent synaptic interconnection systems and brain-like chips (summarized in Fig. 12).

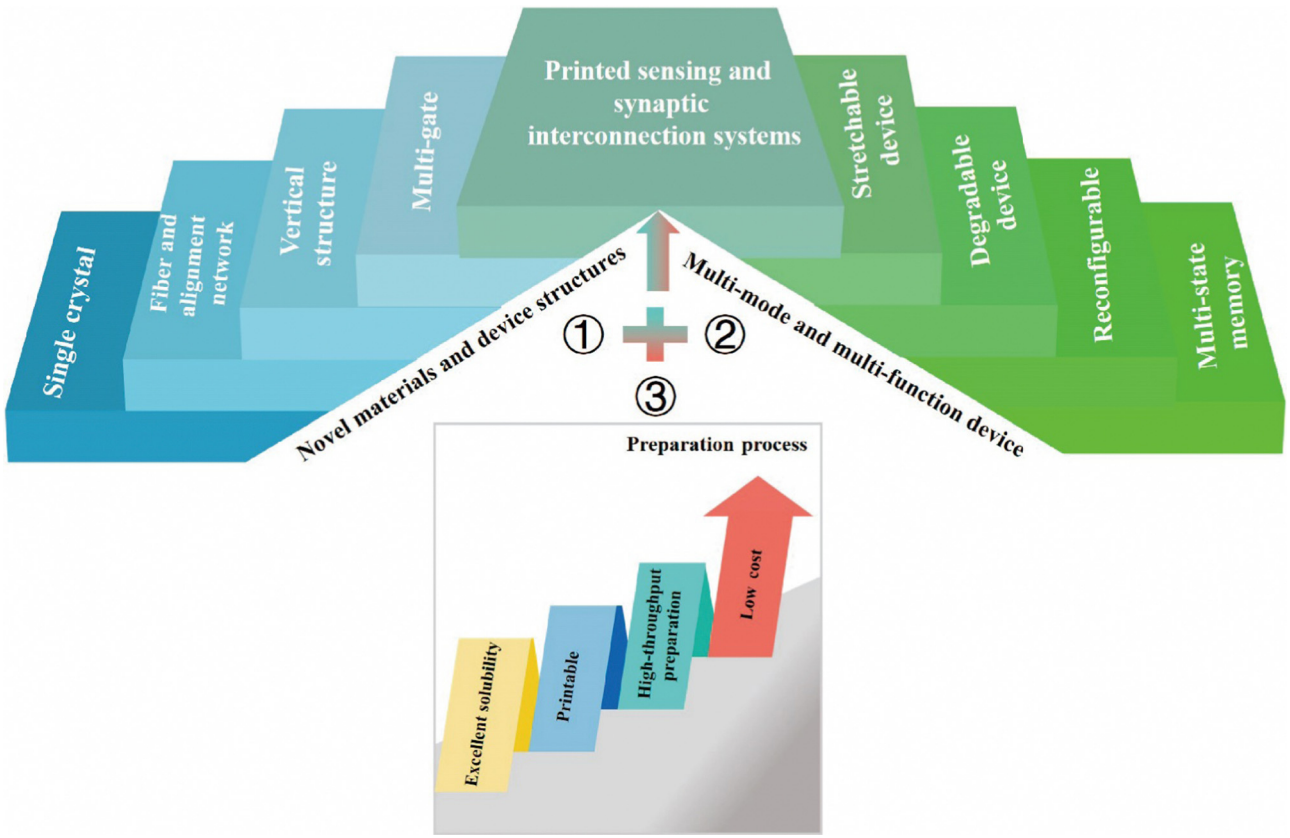

Fig. 12 Summary and outlook of this review from the innovative structural design of materials, special device structural design and processing processes.

While the next wave of transistor-based synaptic electronic systems is on the horizon, challenges and opportunities still exist and need to be addressed.

5.1. The challenges

(1) There are relatively few studies related to multi-mode and reconfigurable synapse properties based on individual transistors, whose multi-stable current states need to be maintained by controlling the carrier in the channel.

(2) The selection of material systems and the integration of low temperature printing processes are urgently needed for e-skin synapse applications.

(3) Complex synaptic system integration and artificial neural network simulation procedures need to be deeply studied and connected.

(4) The multi-signal simulation principles of neural network interconnected systems need to be further explored.

Based on the proposed challenges, there are also many opportunities to further improve the development of intelligent synapses.

5.2. The opportunities

(1) The preparation of multimodal reconfigurable and low power consumption synaptic transistors can be effectively facilitated by controlling the carrier capture and induction processes.

(2) Preparation of fully printed stretchable synaptic transistors using material blending systems such as organic polymers and carbon nanotubes to increase viscosity suitable for printing processes.

(3) Development of high density integrated synaptic transistor systems driven by multiple sensing coupling interconnects.

(4) Implantable fully degradable synaptic transistor interconnect system possessing promising applications.

More generally, future research should consider the potential effects of muti-mode, reconfigurable, flexible, printable, fully degradable, stretchable and system-integrated capabilities more carefully. Under this context, it believes that multidisciplinary cross-collaborative research will enable the successful fabrication and application of numerous synaptic electronic systems in the future.

Author contributions

Xin Wang: investigation, artical analysis, writing original draft. Yixin Ran: investigation, writing part of the original draft. Xiaoqian Li: revision of the manuscript. Xinsu Qin: investigation. Wanlong Lu: correction. Yuanwei Zhu: editing. Guanghao Lu: editing, funding acquisition.

Conflicts of interest

There are no conflicts to declare.

Acknowledgements

This work was financially supported by the National Natural Science Foundation of China (Grant No. 51873172, 51907148 and 52273026), and the Key Scientific and Technological Innovation Team Project of Shaanxi Province (2021GXLH-Z-055). G. L. thanks the support of the Cyrus Tang Foundation, and the Key Scientific and Technological Innovation Team Project of Shanxi Province (2020TD-002).

References

1 G. Indiveri and S.-C. Liu, *Proc. IEEE*, 2015, **103**, 1379–1397.
2 P. Feng, W. Xu, Y. Yang, X. Wan, Y. Shi, Q. Wan, J. Zhao and Z. Cui, *Adv. Funct. Mater.*, 2017, **27**, 1604447.
3 R. W. Picard, E. Vyzas and J. Healey, *IEEE Trans. Pattern Anal. Mach. Intell.*, 2001, **23**, 1175–1191.
4 S. Furber, *J. Neural Eng.*, 2016, **13**, 051001.
5 R. A. Sporea, K. M. Niang, A. J. Flewitt and S. R. P. Silva, *Adv. Mater.*, 2019, **31**, 1902551.
6 B. M. Yu, *Nature*, 2016, **532**, 449–450.
7 Q. Guo, J. Koo, Z. Xie, R. Avila, X. Yu, X. Ning, H. Zhang, X. Liang, S. B. Kim, Y. Yan, M. R. MacEwan, H. M. Lee, A. Song, Z. Di, Y. Huang, Y. Mei and J. A. Rogers, *Adv. Funct. Mater.*, 2019, **29**, 1905451.
8 F. Molina-Lopez, T. Z. Gao, U. Kraft, C. Zhu, T. Öhlund, R. Pfattner, V. R. Feig, Y. Kim, S. Wang, Y. Yun and Z. Bao, *Nat. Commun.*, 2019, **10**, 2676.
9 H. Shim, F. Ershad, S. Patel, Y. Zhang, B. Wang, Z. Chen, T. J. Marks, A. Facchetti and C. Yu, *Nat. Electron.*, 2022, **5**, 670–671.
10 C. Qian, Y. Choi, Y. J. Choi, S. Kim, Y. Y. Choi, D. G. Roe, M. S. Kang, J. Sun and J. H. Cho, *Adv. Mater.*, 2020, **32**, 2002653.
11 L. Liu, Y. Ni, J. Liu, Y. Wang, C. Jiang and W. Xu, *Adv. Funct. Mater.*, 2023, **33**, 2210119.
12 J. Gong, H. Wei, J. Liu, L. Sun, Z. Xu, H. Huang and W. Xu, *Matter*, 2022, **5**, 1578–1589.
13 *Nat. Electron.*, 2020, **3**, 347, DOI: **10.1038/s41928-020-0457-1**.
14 Y. Hu, M. Dai, W. Feng, X. Zhang, F. Gao, S. Zhang, B. Tan, J. Zhang, Y. Shuai, Y. Fu and P. Hu, *Adv. Mater.*, 2021, **33**, 2104960.
15 J. Wang, J. Wang, J. Zhang, W. Huang, X. Wang and M. Zhang, *Adv. Electron. Mater.*, 2022, **8**, 2100922.
16 R. Martins, A. Nathan, R. Barros, L. Pereira, P. Barquinha, N. Correia, R. Costa, A. Ahnood, I. Ferreira and E. Fortunato, *Adv. Mater.*, 2011, **23**, 4491–4496.
17 J. Wang, X. Guo, Z. Yu, Z. Ma, Y. Liu, Z. Lin, M. Chan, Y. Zhu, X. Wang and Y. Chai, *Adv. Funct. Mater.*, 2020, **30**, 2003859.
18 X. Wang, M. Zhu, X. Li, Z. Qin, G. Lu, J. Zhao and Z. Zhang, *Adv. Mater.*, 2022, **34**, 2204066.
19 M. M. Waldrop, *Nat. News*, 2016, **530**, 144.
20 V. Balasubramanian, *Proc. Natl. Acad. Sci. U. S. A.*, 2021, **118**, e2107022118.

21 X. Wang, W. Lu, P. Wei, Z. Qin, N. Qiao, X. Qin, M. Zhang, Y. Zhu, L. Bu and G. Lu, *ACS Appl. Mater. Interfaces*, 2022, **14**, 48948–48959.
22 Y. Shen, N. C. Harris, S. Skirlo, M. Prabhu, T. Baehr-Jones, M. Hochberg, X. Sun, S. Zhao, H. Larochelle, D. Englund and M. Soljačić, *Nat. Photonics*, 2017, **11**, 441–446.
23 I. Cong, S. Choi and M. D. Lukin, *Nat. Phys.*, 2019, **15**, 1273–1278.
24 T. Zhao, Y. Han, L. Qin, H. Guan, L. Xing, X. Li, X. Xue, G. Li and Y. Zhan, *Nano Energy*, 2021, **85**, 106006.
25 X. Xiao, Y. Fang, X. Xiao, J. Xu and J. Chen, *ACS Nano*, 2021, **15**, 18633–18646.
26 J.-Q. Yang, R. Wang, Y. Ren, J.-Y. Mao, Z.-P. Wang, Y. Zhou and S.-T. Han, *Adv. Mater.*, 2020, **32**, 2003610.
27 Z. Cheng, C. Rios, W. H. P. Pernice, C. D. Wright and H. Bhaskaran, *Sci. Adv.*, 2017, **3**, e1700160.
28 X. Ji, B. D. Paulsen, G. K. K. Chik, R. Wu, Y. Yin, P. K. L. Chan and J. Rivnay, *Nat. Commun.*, 2021, **12**, 2480.
29 K. Liang, R. Wang, B. Huo, H. Ren, D. Li, Y. Wang, Y. Tang, Y. Chen, C. Song, F. Li, B. Ji, H. Wang and B. Zhu, *ACS Nano*, 2022, **16**, 8651–8661.
30 S. Kim, B. Choi, M. Lim, J. Yoon, J. Lee, H.-D. Kim and S.-J. Choi, *ACS Nano*, 2017, **11**, 2814–2822.
31 M. Hu, J. Yu, Y. Chen, S. Wang, B. Dong, H. Wang, Y. He, Y. Ma, F. Zhuge and T. Zhai, *Mater. Horiz.*, 2022, **9**, 2335–2344.
32 K. Wang, S. Dai, Y. Zhao, Y. Wang, C. Liu and J. Huang, *Small*, 2019, **15**, 1900010.
33 J. Choi, J. S. Han, K. Hong, S. Y. Kim and H. W. Jang, *Adv. Mater.*, 2018, **30**, 1704002.
34 C. Giotis, A. Serb, V. Manouras, S. Stathopoulos and T. Prodromakis, *Sci. Adv.*, 2022, **8**, eabn7920.
35 H. Wang, Q. Zhao, Z. Ni, Q. Li, H. Liu, Y. Yang, L. Wang, Y. Ran, Y. Guo, W. Hu and Y. Liu, *Adv. Mater.*, 2018, **30**, 1803961.
36 B. Yang, Y. Wang, Z. Hua, J. Zhang, L. Li, D. Hao, P. Guo, L. Xiong and J. Huang, *Chem. Commun.*, 2021, **57**, 8300–8303.
37 D. Yang, H. Yang, X. Guo, H. Zhang, C. Jiao, W. Xiao, P. Guo, Q. Wang and D. He, *Adv. Funct. Mater.*, 2020, **30**, 2004514.
38 N. He, F. Ye, J. Liu, T. Sun, X. Wang, W. Hou, W. Shao, X. Wan, Y. Tong, F. Xu and Y. Sheng, *Adv. Electron. Mater.*, 2023, **9**, 2201038.
39 H. Yu, H. Wei, J. Gong, H. Han, M. Ma, Y. Wang and W. Xu, *Small*, 2021, **17**, 2000041.
40 X. Li, Y. Liu, J. Zhang, F. Wu, M. Hu and H. Yang, *Adv. Intelligent Syst.*, 2022, **4**, 2200015.
41 S. Dai, Y. Zhao, Y. Wang, J. Zhang, L. Fang, S. Jin, Y. Shao and J. Huang, *Adv. Funct. Mater.*, 2019, **29**, 1903700.
42 C. Eckel, J. Lenz, A. Melianas, A. Salleo and R. T. Weitz, *Nano Lett.*, 2022, **22**, 973–978.
43 T. Chen, X. Wang, D. Hao, S. Dai, Q. Ou, J. Zhang and J. Huang, *Adv. Opt. Mater.*, 2021, **9**, 2002030.
44 G. Liu, Q. Li, W. Shi, Y. Liu, K. Liu, X. Yang, M. Shao, A. Guo, X. Huang, F. Zhang, Z. Zhao, Y. Guo and Y. Liu, *Adv. Funct. Mater.*, 2022, **32**, 2200959.
45 Y.-S. Zhang, B.-J. Chen, X. Deng, Z. Guan, B.-B. Chen, Y. Chen, N. Zhong, P.-H. Xiang and C.-G. Duan, *J. Mater. Chem. C*, 2022, **10**, 11654–11663.
46 L. Danial, E. Pikhay, E. Herbelin, N. Wainstein, V. Gupta, N. Wald, Y. Roizin, R. Daniel and S. Kvatinsky, *Nat. Electron.*, 2019, **2**, 596–605.
47 Y. Zhu, Y. Fan, S. Li, P. Wei, D. Li, B. Liu, D. Cui, Z. Zhang, G. Li, Y. Nie and G. Lu, *Mater. Horiz.*, 2020, **7**, 1861–1871.
48 Z.-D. Luo, X. Xia, M.-M. Yang, N. R. Wilson, A. Gruverman and M. Alexe, *ACS Nano*, 2020, **14**, 746–754.
49 Y. Yang, R. C. da Costa, M. J. Fuchter and A. J. Campbell, *Nat. Photonics*, 2013, **7**, 634–638.
50 M. E. Beck, A. Shylendra, V. K. Sangwan, S. Guo, W. A. Gaviria Rojas, H. Yoo, H. Bergeron, K. Su, A. R. Trivedi and M. C. Hersam, *Nat. Commun.*, 2020, **11**, 1565.
51 Y. Lee, J. Y. Oh, W. Xu, O. Kim, T. R. Kim, J. Kang, Y. Kim, D. Son, J. B.-H. Tok, M. J. Park, Z. Bao and T.-W. Lee, *Sci. Adv.*, 2018, **4**, eaat7387.
52 S. Zhang, E. Hubis, G. Tomasello, G. Soliveri, P. Kumar and F. Cicoira, *Chem. Mater.*, 2017, **29**, 3126–3132.
53 Y. Dai, H. Hu, M. Wang, J. Xu and S. Wang, *Nat. Electron.*, 2021, **4**, 17–29.
54 Z. Bao and X. Chen, *Adv. Mater.*, 2016, **28**, 4177–4179.
55 S. Zhang and W. Xu, *J. Mater. Chem. C*, 2020, **8**, 11138–11144.
56 L. Li, K. Wang, H. Fan, X. Zhu, J. Mu, H. Yu, Q. Zhang, Y. Li, C. Hou and H. Wang, *Mater. Horiz.*, 2021, **8**, 1711–1721.
57 Y. Jiang and B. Tian, *Nat. Rev. Mater.*, 2018, **3**, 473–490.
58 M. Cai, X. Tong, H. Zhao, X. Li, Y. You, R. Wang, L. Xia, N. Zhou, L. Wang and Z. M. Wang, *Small*, 2022, **18**, 2204495.
59 Y. Yang, X. Zhao, C. Zhang, Y. Tong, J. Hu, H. Zhang, M. Yang, X. Ye, S. Wang, Z. Sun, Q. Tang and Y. Liu, *Adv. Funct. Mater.*, 2020, **30**, 2006271.
60 B. Yang, Y. Lu, D. Jiang, Z. Li, Y. Zeng, S. Zhang, Y. Ye, Z. Liu, Q. Ou, Y. Wang, S. Dai, Y. Yi and J. Huang, *Adv. Mater.*, 2020, **32**, 2001227.
61 S. Dai, X. Wu, D. Liu, Y. Chu, K. Wang, B. Yang and J. Huang, *ACS Appl. Mater. Interfaces*, 2018, **10**, 21472–21480.
62 J. Li, W. Fu, Y. Lei, L. Li, W. Zhu and J. Zhang, *ACS Appl. Mater. Interfaces*, 2022, **14**, 8587–8597.
63 H. Lian, Q. Liao, B. Yang, Y. Zhai, S.-T. Han and Y. Zhou, *J. Mater. Chem. C*, 2021, **9**, 640–648.
64 X. Deng, S.-Q. Wang, Y.-X. Liu, N. Zhong, Y.-H. He, H. Peng, P.-H. Xiang and C.-G. Duan, *Adv. Funct. Mater.*, 2021, **31**, 2101099.
65 D. Choi, M.-K. Song, T. Sung, S. Jang and J.-Y. Kwon, *Nano Energy*, 2020, **74**, 104912.
66 H. Wei, Y. Ni, L. Sun, H. Yu, J. Gong, Y. Du, M. Ma, H. Han and W. Xu, *Nano Energy*, 2021, **81**, 105648.
67 S. Seo, S.-H. Jo, S. Kim, J. Shim, S. Oh, J.-H. Kim, K. Heo, J.-W. Choi, C. Choi, S. Oh, D. Kuzum, H.-S. P. Wong and J.-H. Park, *Nat. Commun.*, 2018, **9**, 5106.
68 C. Jiang, J. Liu, L. Yang, J. Gong, H. Wei and W. Xu, *Adv. Sci.*, 2022, **9**, 2106124.

69 I. Krauhausen, D. A. Koutsouras, A. Melianas, S. T. Keene, K. Lieberth, H. Ledanseur, R. Sheelamanthula, A. Giovannitti, F. Torricelli, I. Mcculloch, P. W. M. Blom, A. Salleo, Y. van de Burgt and P. Gkoupidenis, *Sci. Adv.*, 2021, **7**, eabl5068.
70 X. Zhao, S. Wang, Y. Ni, Y. Tong, Q. Tang and Y. Liu, *Adv. Sci.*, 2021, **8**, 2004050.
71 J. Kim, Y. Kim, O. Kwon, T. Kim, S. Oh, S. Jin, W. Park, J.-D. Kwon, S.-W. Hong, C.-S. Lee, H.-Y. Ryu, S. Hong, J. Kim, T.-Y. Heo and B. Cho, *Adv. Electron. Mater.*, 2020, **6**, 1901072.
72 C. Wang, W.-Y. Lee, D. Kong, R. Pfattner, G. Schweicher, R. Nakajima, C. Lu, J. Mei, T. H. Lee, H.-C. Wu, J. Lopez, Y. Diao, X. Gu, S. Himmelberger, W. Niu, J. R. Matthews, M. He, A. Salleo, Y. Nishi and Z. Bao, *Sci. Rep.*, 2015, **5**, 17849.
73 W. Huang, P. Hang, Y. Wang, K. Wang, S. Han, Z. Chen, W. Peng, Y. Zhu, M. Xu, Y. Zhang, Y. Fang, X. Yu, D. Yang and X. Pi, *Nano Energy*, 2020, **73**, 104790.
74 S. J. Kim, J.-S. Jeong, H. W. Jang, H. Yi, H. Yang, H. Ju and J. A. Lim, *Adv. Mater.*, 2021, **33**, 2100475.
75 Y. Choi, S. Oh, C. Qian, J.-H. Park and J. H. Cho, *Nat. Commun.*, 2020, **11**, 4595.
76 H. Shim, K. Sim, F. Ershad, P. Yang, A. Thukral, Z. Rao, H.-J. Kim, Y. Liu, X. Wang, G. Gu, L. Gao, X. Wang, Y. Chai and C. Yu, *Sci. Adv.*, 2019, **5**, eaax4961.
77 H. Wang, Y. Chen, Z. Ni and P. Samorì, *Adv. Mater.*, 2022, **34**, 2205945.
78 L. Liu, W. Xu, Y. Ni, Z. Xu, B. Cui, J. Liu, H. Wei and W. Xu, *ACS Nano*, 2022, **16**, 2282–2291.
79 X. Huang, Y. Liu, G. Liu, K. Liu, X. Wei, M. Zhu, W. Wen, Z. Zhao, Y. Guo and Y. Liu, *Adv. Funct. Mater.*, 2023, **33**, 2208836.
80 J. Tang, C. He, J. Tang, K. Yue, Q. Zhang, Y. Liu, Q. Wang, S. Wang, N. Li, C. Shen, Y. Zhao, J. Liu, J. Yuan, Z. Wei, J. Li, K. Watanabe, T. Taniguchi, D. Shang, S. Wang, W. Yang, R. Yang, D. Shi and G. Zhang, *Adv. Funct. Mater.*, 2021, **31**, 2011083.
81 M. Xu, X. Mai, J. Lin, W. Zhang, Y. Li, Y. He, H. Tong, X. Hou, P. Zhou and X. Miao, *Adv. Funct. Mater.*, 2020, **30**, 2003419.
82 Q. Zhang, T. Jin, X. Ye, D. Geng, W. Chen and W. Hu, *Adv. Funct. Mater.*, 2021, **31**, 2106151.
83 S. G. J. Mathijssen, M.-J. Spijkman, A.-M. Andringa, P. A. van Hal, I. McCulloch, M. Kemerink, R. A. J. Janssen and D. M. de Leeuw, *Adv. Mater.*, 2010, **22**, 5105–5109.
84 J. Zhang, T. Sun, S. Zeng, D. Hao, B. Yang, S. Dai, D. Liu, L. Xiong, C. Zhao and J. Huang, *Nano Energy*, 2022, **95**, 106987.
85 J. Yu, Y. Wang, S. Qin, G. Gao, C. Xu, Z. Lin Wang and Q. Sun, *Mater. Today*, 2022, **60**, 158–182.
86 J. Shi, S. D. Ha, Y. Zhou, F. Schoofs and S. Ramanathan, *Nat. Commun.*, 2013, **4**, 2676.
87 J.-K. Qin, F. Zhou, J. Wang, J. Chen, C. Wang, X. Guo, S. Zhao, Y. Pei, L. Zhen, P. D. Ye, S. P. Lau, Y. Zhu, C.-Y. Xu and Y. Chai, *ACS Nano*, 2020, **14**, 10018–10026.
88 S.-K. Lee, Y. W. Cho, J.-S. Lee, Y.-R. Jung, S.-H. Oh, J.-Y. Sun, S. Kim and Y.-C. Joo, *Adv. Sci.*, 2021, **8**, 2001544.
89 C. Zhang, S. Wang, X. Zhao, Y. Yang, Y. Tong, M. Zhang, Q. Tang and Y. Liu, *Adv. Funct. Mater.*, 2021, **31**, 2007894.
90 S.-H. Kim and W.-J. Cho, *Polymers*, 2022, **14**, 1372.
91 H.-S. Kim, H. Park and W.-J. Cho, *Nanomaterials*, 2022, **12**, 2596.
92 R. Wang, P. Chen, D. Hao, J. Zhang, Q. Shi, D. Liu, L. Li, L. Xiong, J. Zhou and J. Huang, *ACS Appl. Mater. Interfaces*, 2021, **13**, 43144–43154.
93 H. R. Lee, D. Lee and J. H. Oh, *Adv. Mater.*, 2021, **33**, 2100119.
94 M. Li, Q. Shu, X. Qing, J. Wu, Q. Xiao, K. Jia, X. Wang and D. Wang, *J. Mater. Chem. C*, 2023, **11**, 5208–5216.
95 D. Kireev, S. Liu, H. Jin, T. Patrick Xiao, C. H. Bennett, D. Akinwande and J. A. C. Incorvia, *Nat. Commun.*, 2022, **13**, 4386.
96 R. Liu, L. Q. Zhu, W. Wang, X. Hui, Z. P. Liu and Q. Wan, *J. Mater. Chem. C*, 2016, **4**, 7744–7750.
97 Y. Yang, X. Zhao, S. Wang, C. Zhang, H. Sun, F. Xu, Y. Tong, Q. Tang and Y. Liu, *J. Mater. Chem. C*, 2020, **8**, 16542–16550.
98 Y. Ke, R. Yu, S. Lan, L. He, Y. Yan, H. Yang, L. Shan, H. Chen and T. Guo, *J. Mater. Chem. C*, 2021, **9**, 4854–4861.
99 S. Wang, C. Chen, Z. Yu, Y. He, X. Chen, Q. Wan, Y. Shi, D. W. Zhang, H. Zhou, X. Wang and P. Zhou, *Adv. Mater.*, 2019, **31**, 1806227.
100 S. Iqbal, L. T. Duy, H. Kang, R. Singh, M. Kumar, J. Park and H. Seo, *Adv. Funct. Mater.*, 2021, **31**, 2102567.
101 M.-K. Kim and J.-S. Lee, *Adv. Mater.*, 2020, **32**, 1907826.
102 P. C. Harikesh, C.-Y. Yang, D. Tu, J. Y. Gerasimov, A. M. Dar, A. Armada-Moreira, M. Massetti, R. Kroon, D. Bliman, R. Olsson, E. Stavrinidou, M. Berggren and S. Fabiano, *Nat. Commun.*, 2022, **13**, 901.
103 G. Cao, P. Meng, J. Chen, H. Liu, R. Bian, C. Zhu, F. Liu and Z. Liu, *Adv. Funct. Mater.*, 2021, **31**, 2005443.
104 J. Xu, S. Wang, G.-J. N. Wang, C. Zhu, S. Luo, L. Jin, X. Gu, S. Chen, V. R. Feig, J. W. F. To, S. Rondeau-Gagné, J. Park, B. C. Schroeder, C. Lu, J. Y. Oh, Y. Wang, Y.-H. Kim, H. Yan, R. Sinclair, D. Zhou, G. Xue, B. Murmann, C. Linder, W. Cai, J. B.-H. Tok, J. W. Chung and Z. Bao, *Science*, 2017, **355**, 59–64.
105 D. H. Park, H. W. Park, J. W. Chung, K. Nam, S. Choi, Y. S. Chung, H. Hwang, B. Kim and D. H. Kim, *Adv. Funct. Mater.*, 2019, **29**, 1808909.
106 S. Wang, J. Xu, W. Wang, G.-J. N. Wang, R. Rastak, F. Molina-Lopez, J. W. Chung, S. Niu, V. R. Feig, J. Lopez, T. Lei, S.-K. Kwon, Y. Kim, A. M. Foudeh, A. Ehrlich, A. Gasperini, Y. Yun, B. Murmann, J. B.-H. Tok and Z. Bao, *Nature*, 2018, **555**, 83–88.
107 Q. Yang, Z.-D. Luo, D. Zhang, M. Zhang, X. Gan, J. Seidel, Y. Liu, Y. Hao and G. Han, *Adv. Funct. Mater.*, 2022, **32**, 202207290.
108 S. M. Kwon, S. W. Cho, M. Kim, J. S. Heo, Y.-H. Kim and S. K. Park, *Adv. Mater.*, 2019, **31**, 1906433.
109 K. Lu, X. Li, Q. Sun, X. Pang, J. Chen, T. Minari, X. Liu and Y. Song, *Mater. Horiz.*, 2021, **8**, 447–470.

110 H. Ling, D. A. Koutsouras, S. Kazemzadeh, Y. van de Burgt, F. Yan and P. Gkoupidenis, *Appl. Phys. Rev.*, 2020, **7**, 011307.
111 K. Liu, Y. Bian, J. Kuang, X. Huang, Y. Li, W. Shi, Z. Zhu, G. Liu, M. Qin, Z. Zhao, X. Li, Y. Guo and Y. Liu, *Adv. Mater.*, 2022, **34**, 2107304.
112 Y. Wang, D. Liu, Y. Zhang, L. Fan, Q. Ren, S. Ma and M. Zhang, *ACS Nano*, 2022, **16**, 8283–8293.
113 X. Wang, Y. Yan, E. Li, Y. Liu, D. Lai, Z. Lin, Y. Liu, H. Chen and T. Guo, *Nano Energy*, 2020, **75**, 104952.
114 X. Wang, E. Li, Y. Liu, S. Lan, H. Yang, Y. Yan, L. Shan, Z. Lin, H. Chen and T. Guo, *Nano Energy*, 2021, **90**, 106497.
115 Q. Ou, B. Yang, J. Zhang, D. Liu, T. Chen, X. Wang, D. Hao, Y. Lu and J. Huang, *Small*, 2021, **17**, 2007241.
116 Y. Li, C. Zhang, X. Zhao, Y. Tong, Q. Tang and Y. Liu, *ACS Appl. Electron. Mater.*, 2022, **4**, 316–325.
117 Y. Yao, X. Huang, S. Peng, D. Zhang, J. Shi, G. Yu, Q. Liu and Z. Jin, *Adv. Electron. Mater.*, 2019, **5**, 1800887.
118 K. Toprasertpong, M. Takenaka and S. Takagi, *Appl. Phys. A: Mater. Sci. Process.*, 2022, **128**, 1114.
119 W. Jie and J. Hao, *Nanoscale*, 2017, **10**, 328–335.
120 C. Zhang, K. Wang, F. Zhao, R. Pan, J. Zhang, H. Yu and J. Li, *Nano Energy*, 2020, **78**, 105324.
121 A. A. Pil'nik, A. A. Chernov and D. R. Islamov, *Sci. Rep.*, 2020, **10**, 15759.
122 P. Wei, X. Wang, X. Li, S. Han, N. Qiao, P. Zhang, Y. Deng, W. Zhang, L. Bu and G. Lu, *Adv. Funct. Mater.*, 2021, **31**, 2103369.
123 Z. Wang, X. Liu, X. Zhou, Y. Yuan, K. Zhou, D. Zhang, H. Luo and J. Sun, *Adv. Mater.*, 2022, **34**, 2200032.
124 Z. Chen, R. Yu, X. Yu, E. Li, C. Wang, Y. Liu, T. Guo and H. Chen, *ACS Nano*, 2022, **16**, 19155–19164.
125 J. Shi, J. Jie, W. Deng, G. Luo, X. Fang, Y. Xiao, Y. Zhang, X. Zhang and X. Zhang, *Adv. Mater.*, 2022, **34**, 2200380.
126 Y. Li, J. Wang, Q. Yang and G. Shen, *Adv. Sci.*, 2022, **9**, 2202123.
127 H. Yu, X. Zhao, M. Tan, B. Wang, M. Zhang, X. Wang, S. Guo, Y. Tong, Q. Tang and Y. Liu, *Adv. Funct. Mater.*, 2022, **32**, 2206765.
128 Y. Kim, A. Chortos, W. Xu, Y. Liu, J. Y. Oh, D. Son, J. Kang, A. M. Foudeh, C. Zhu, Y. Lee, S. Niu, J. Liu, R. Pfattner, Z. Bao and T.-W. Lee, *Science*, 2018, **360**, 998–1003.
129 C. Wan, G. Chen, Y. Fu, M. Wang, N. Matsuhisa, S. Pan, L. Pan, H. Yang, Q. Wan, L. Zhu and X. Chen, *Adv. Mater.*, 2018, **30**, 1801291.
130 Y. Liu, J. Zhong, E. Li, H. Yang, X. Wang, D. Lai, H. Chen and T. Guo, *Nano Energy*, 2019, **60**, 377–384.
131 H. Wan, Y. Cao, L.-W. Lo, J. Zhao, N. Sepulveda and C. Wang, *ACS Nano*, 2020, **14**, 10402–10412.
132 Y. R. Lee, T. Q. Trung, B.-U. Hwang and N.-E. Lee, *Nat. Commun.*, 2020, **11**, 2753.
133 R. Yu, Y. Yan, E. Li, X. Wu, X. Zhang, J. Chen, Y. Hu, H. Chen and T. Guo, *Mater. Horiz.*, 2021, **8**, 2797–2807.
134 F. Sun, Q. Lu, M. Hao, Y. Wu, Y. Li, L. Liu, L. Li, Y. Wang and T. Zhang, *npj Flex Electron*, 2022, **6**, 1–8.

